Journal of Power Sources 233 (2013) 216–230

Contents lists available at SciVerse ScienceDirect

Journal of Power Sources

journal homepage: www.elsevier.com/locate/jpowsour

Review

Physical and chemical modification routes leading to improved mechanical properties of perfluorosulfonic acid membranes for PEM fuel cells

Surya Subianto [a,*], Monica Pica [b], Mario Casciola [b], Paula Cojocaru [c], Luca Merlo [c], Graham Hards [d], Deborah J. Jones [a,**]

[a] Institut Charles Gerhardt, UMR 5253 CNRS, Agrégats, Interfaces et Matériaux pour l'Energie, Université Montpellier 2, Montpellier, France
[b] Dipartimento di Chimica, Università di Perugia, Perugia, Italy
[c] Solvay Specialty Polymers, Viale Lombardia 20, Bollate (MI), Italy
[d] Johnson Matthey Fuel Cells PLC, Blounts Court, Sonning Common, Reading, UK

HIGHLIGHTS

- Approaches to improving membrane stability are critically assessed.
- Consideration given to both mechanical and chemical stabilisation.
- Ionomer cross-linking, inorganic-organic composite and reinforced membranes.

ARTICLE INFO

Article history:
Received 8 October 2012
Received in revised form
10 December 2012
Accepted 14 December 2012
Available online 16 February 2013

Keywords:
Fuel cell membrane
Mechanical properties
Perfluorosulfonic acid
Reinforcement
Composite
Cross-linking

ABSTRACT

Proton Exchange Membrane Fuel Cells (PEMFC) are a sustainable means of power generation through electrochemical conversion of hydrogen-containing fuels especially in portable, stationary, and automotive applications. In order to improve fuel cell performance and durability as well as reduce material cost, significant research effort has been dedicated to enhancing the mechanical properties of perfluorosulfonic acid (PFSA) membranes used in PEMFCs as this allows the use of thinner membranes, which significantly reduces area resistance and improves water management in the fuel cell. This review looks at various approaches to improve the mechanical properties of PFSA membranes, from chemical methods such as cross-linking to the use of a physical reinforcement in various forms such as porous polymer matrix, fibres, or inorganic reinforcement.

1. Introduction

Proton Exchange Membrane Fuel Cells (PEMFC) are an attractive, sustainable means for power generation. However, the cost of the cell components and the need to increase fuel cell long-term durability still preclude the immediate and large-scale commercialisation of fuel cell technologies especially in highly demanding applications such as automotives. Perfluorosulfonic acid (PFSA) membranes such as Nafion® from DuPont™ have long been regarded as state-of-the-art membranes for PEMFCs due to their high proton conductivity and chemical stability [1]. In the past, the mechanical properties of fuel cell membranes have not been of the most critical importance [2], principally because initial efforts used thicker (50–200 μm) membranes. However, recent developments have been geared towards the use of thinner membranes (<50 μm) due to the advantages they confer (such as lower membrane resistance and improved water transport) and, considering the various stresses they have to withstand during operation, improvement in membrane mechanical properties becomes an important goal in order to increase resistance

* Corresponding author. ICG-AIME, Université Montpellier 2, Place Eugene Bataillon, Montpellier, France. Tel.: +33 467 14 90 98; fax: +33 0 467 14 33 04.
** Corresponding author. ICG-AIME, Université Montpellier 2, Place Eugene Bataillon, Montpellier, France. Tel.: +33 467 14 33 30; fax: +33 0 467 14 33 04.
E-mail addresses: surya.subianto@univ-montp2.fr (S. Subianto), Deborah.Jones@univ-montp2.fr (D.J. Jones).

0378-7753/$ – see front matter © 2013 Elsevier B.V. All rights reserved.
http://dx.doi.org/10.1016/j.jpowsour.2012.12.121

of the membrane to premature failure. In an operating fuel cell the membrane has to withstand chemical degradation due to attack by radicals and other reactive species as well as mechanical stresses caused by swelling and dehydration or variation in stack compression. When one considers the importance of membrane durability to the MEA lifetime, improving their mechanical properties becomes an important goal in order to increase the membrane's resistance to failure. Thus, although membrane degradation is a result of both chemical and mechanical effects, the mechanical properties of the membrane remain a metric by which its potential resistance to failure can be gauged [3]. In particular, failure stress and tear resistance can serve as indicators of MEA lifetime as they are sensitive to localised mechanical and chemical degradation of the membrane [4].

2. Mechanical properties of PFSA membranes and their durability

2.1. Mechanical properties of PFSA

The mechanical properties of commercially available membranes such as Nafion® are generally available in the product literature (Table 1), with properties such as tensile modulus, breaking strength, and elongation at yield typically measured under ambient conditions and 50%RH. Aside from this, much of the literature has been directed more towards identifying thermomechanical transitions that can be assigned to morphological features using techniques such as Dynamic Mechanical Analysis (DMA).

An early study [5] of the loss tangent ($\tan\delta$) and storage tensile modulus (E′) of Nafion® shows a transition around 110 °C, labelled as the α transition which was initially considered as the glass transition of the non-ionic phase as it was not significantly affected by water content. Later studies and correlations with other data from SAXS and molecular dynamics reattributed this transition to the onset of long-range chain mobility as a result of a destabilisation of the electrostatic network [6]. A β peak, centred around 20 °C, is associated with the onset of segmental motions of chains within the framework of a static network of a physically cross-linked chains [7], while a γ peak at around −100 °C is considered to have the same origin as in PTFE, namely due to short-range molecular motion in the non-ionic phase [2].

Other studies have placed greater importance on hydration, as water produces a significant plasticizing effect on the PFSA membrane [8] and induces morphological changes [9] which can significantly affect its mechanical properties. Hydrothermal stresses alone are capable of causing gas crossover failure in PEMFCs, with a linear relationship between hydrothermal expansion and water content. The modulus of the material decreases as RH increases, and viscoelastic flow under compression resulted in shrinkage, which later manifests itself as tensile stresses [10].

Due to the complexity of the factors contributing to membrane degradation and variable nature of the fuel cell environment, no single property can be used as a stand-alone metric for membrane durability. In an simplified relationship between mechanical properties and durability, mechanical strength decreases over time as a result of chemical and physical degradation, until eventually it crosses a threshold at which breaching occurs. However, the exact nature of membrane failure is a result of various variables including material properties, assembly, and operating conditions for a given MEA. The effectiveness of membrane stabilisation approaches in the fuel cell environment can be assessed by use of conditions that specifically accelerate ageing, for example by maintaining the MEA at open cell voltage at low relative humidity (chemical degradation), and by cycling between wet and dry conditions (mechanical ageing), with periodic evaluation of membrane integrity by physical leak testing and hydrogen cross-over measurements.

2.2. Failure mechanisms of PFSA membranes due to mechanical degradation

Among the three membrane degradation mechanisms [11,12] (mechanical, chemical, and thermal), mechanical degradation causes early life failures due to perforations, cracks, tears, or pinholes, which can also result from internal defects or improper assembly during MEA fabrication. During fuel cell operation, dimensional changes and the non-uniform mechanical stresses corresponding to the interface between the land and the channels in the flow field are susceptible especially to in-plane stresses (Fig. 1). The resulting mechanical fatigue due to alternating compressive and tensile stresses are responsible for a particular set of membrane failure mechanisms [13]. Blistering [14] can be caused by the growth of voids associated with contaminant particles. These voids are initially filled with water and expand at higher temperatures due to the higher vapour partial pressure within, and then coalesce to form larger voids. Residual swelling-induced in-plane tensile stresses may explain mechanical failures in the form

Table 1
Mechanical properties of several commercially available PFSA membranes.

Membrane	Conditions	Yield strength		Maximum tensile strength (MPa)		Elastic modulus (MPa)		Elongation at break (%)		Ref.
		MD[a]	TD[b]	MD	TD	MD	TD	MD	TD	
Nafion® (N115, N117, N110)	23°C, 50% RH	–		43	32	249		225		[157]
	Water soaked, 23°C	–		34	26	114		200		
	Water soaked, 100°C	–		25	24	64		180		
Nafion® NR-111	23°C, 50% RH	14.4	14.0	30.5	28.0	272	253	253	235	[158]
	80°C, 100% RH	4.4	4.6	8.9	9.5	23.9	25.1	159	188	
IonPower® N111-IP	23°C, 50% RH	14.1	14.9	32.6	37.5	304	319	176	141	
	80°C, 100% RH	5.0	5.3	17.2	16.1	45.0	51.5	193	127	
Aquivion™										
E79-03S	23°C, 50% RH	9–13	9–13	20–40	20–35	–		90	200	[159]
E87-03	23°C, 50% RH	>11	>11	>25	>20	–		140	200	
3M	25°C, 50% RH	–		30.5		–		128		[20]
Gore™ Primea®	23°C, 50% RH	18.0	15.6	35.0	32.3	324	340	196	147	[158]
	80°C, 100% RH	5.2	4.1	18.4	15.1	58.0	28.3	153	157	
Gore-Select®	25°C, 50% RH	19		43	49	560	490	120		[81] [c]

[a] MD = Machine direction.
[b] TD = Transverse direction.
[c] values approximated from graphs provided.

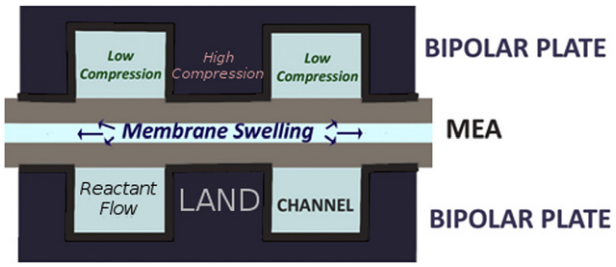

Fig. 1. Stresses experienced by an MEA in a stack.

of cracking or tearing of the membrane as well as delamination at the membrane/electrode interface. Other factors such as mismatch in material properties (and hence their dimensional changes with temperature) can also contribute to mechanical failure, however it has been reported [15] that repetitive freeze thaw cycling, in the absence of other stresses, does not result in catastrophic effect despite a loss in tensile strength (due to changes in polymer chain entanglements).

Compared to thermally induced mechanical stresses, hydration can induce much more significant stresses as nano-scale changes of the morphology of the ionic clusters [16] result in not only a build up in internal stresses, but also a macroscopic dimensional change which can be quite significant. Humidity gradients between the cathode and the anode also lead to swelling anisotropy and greater stresses on the anode side [17,18]. In an MEA, failure location depends strongly on cell configuration, as defects in the form of pinholes, cracks, and delamination are generally localised along low compression area such as the flow channels. These defects can propagate through the membrane, eventually resulting in reactant crossover. Although chemical attack is considered the primary cause of membrane degradation [19], these stresses contribute to accelerate membrane failure by propagating cracks and exposing more of the membrane to chemical degradation. Hence, membrane failure can be a result of the combination of defect formation, reduction of membrane ductility and mechanical strain excursion caused by constrained drying [4].

2.3. Motivations for improving the mechanical properties of PFSA fuel cell membranes

Ex situ stress cycling tests show that membrane failure can occur in the absence of chemical degradation, but in situ effects can further accelerate this degradation by weakening the intrinsic mechanical properties of the membrane and forming new defects such as pinholes. Thus, MEA degradation often manifests as a gradual decay in fuel cell performance due to electrode and catalyst degradation/corrosion, followed by a sudden, catastrophic failure of the cell or stack due to gas crossover through tears in the membrane. In this regard, the ability of the membrane to resist breaching is often the limiting factor in the lifetime of PEMFC cells and stacks, and although the exact relationship between mechanical properties and membrane durability is not known, it is agreed that stronger membranes are needed to achieve the durability and lifetime targets of any given application [20].

Another major motivation to improve the mechanical properties of PFSA membranes is to enable the fabrication of thinner membrane materials. This directly reduces the material cost and also improves water management in the fuel cell through facilitating back diffusion. Importantly also, the use of thinner membranes significantly lowers the electrical resistivity across the membrane, resulting in better fuel cell performance as the reduction of the output voltage of the cell (compared to theoretical values) is mainly due to the IR loss caused by the resistance of the membrane.

In the literature, several approaches have been investigated that can broadly be grouped into those using a chemical method or a physical reinforcement. Chemical reinforcement can be achieved through the modification of the polymer structure, either through side chain or end-chain cross-linking, while physical reinforcement relies on incorporation of a mechanically stable polymer or inorganic support material in various forms (porous membranes, fibres, particles, yarns).

3. Mechanical properties and durability improvements through chemical methods

3.1. Chemical cross-linking

In many types of polymer, chemical cross-linking is an excellent method for increasing mechanical strength [21], and to reduce swelling. As such, cross-linking is a widely used approach in non-fluorinated and also some partially fluorinated polymers when an improvement in mechanical properties is required. However, there is relatively little published work on the cross-linking of PFSA ionomers compared to other polymers, which may be due to the inherent stability of the perfluorinated backbone which results in a lack of readily available cross-linking sites. Thus, the cross-linking of PFSA generally requires either the conversion of the sulfonic acid side chain or the synthesis of a polymer containing cross-linkable functional groups. Nevertheless, a few studies are available on this subject, with various different reaction pathways possible to achieve chemical cross-linking of PFSAs (Fig. 2).

One of the earliest publications in this area was by Covitch et al. [22], who followed an earlier study by Hora et al. [23] on the cross-

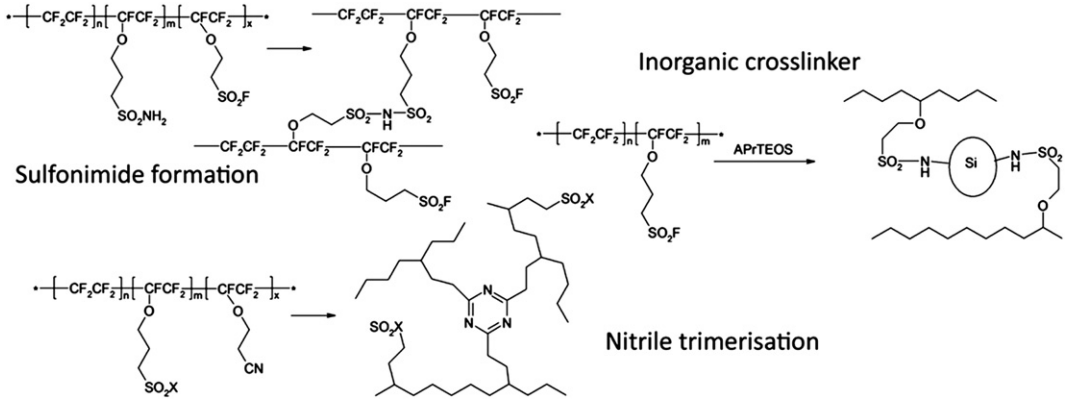

Fig. 2. Schematics of some reaction pathways on the cross-linking of PFSAs [27,30,35].

linking of chemically modified Nafion® 117. This was achieved by converting the sulfonic acid side chains of Nafion® into sulfonyl chloride groups, which were then treated with ethylenediamine to form sulfonamide functionalities. Although in principle the diamines can form cross-links directly with the sulfonyl chloride, it was found that thermal post-treatment was necessary to increase cross-linking as the reaction is diffusion controlled. Another approach to the synthesis of cross-linked PFSA analogues is through the polymerisation of perfluorinated monomers containing cross-linkable groups. Such an approach has been used to prepare perfluorosulfonimide polymers, with sulfonimide groups in place of sulfonic acid groups. The synthesis of perfluoro(sulfonyl)imide polymers has been shown by DesMarteau et al. [24,25], and a study by Savett et al. [26] found similar fuel cell performance for the perfluoro(sulfonyl)imide and Nafion® of a similar equivalent weight. However, in these studies the main purpose of the (sulfonyl)imide functionalities was to improve fuel cell performance as perfluorosulfonyl(imide) is known to possess stronger gas phase acidity and better thermal stability than sulfonic acids, and although they mentioned the possibility of cross-linking these authors did not attempt structural cross-linking of their membranes through chemical modification of the sulfonyl(imide) functionalities.

In a similar approach, Uematsu et al. [27] synthesised a copolymer containing both sulfonamide and sulfonyl fluoride functionalities. Unlike the perfluoro(sulfonyl)imides, these copolymers can react to form sulfonimide cross-links in the presence of triethylamine. As any unreacted sulfonyl fluoride functionality can be converted into sulfonic acid in the post-treatment, the amount of cross-linking sites can be controlled through the quantity of sulfonamide functionalities in the polymer. Interestingly, the conductivity of the cross-linked and non-cross-linked membranes was the same, which was attributed to the sulfonimide group acting as a super acid, thus maintaining the overall concentration of protogenic groups.

Zhang et al. [28] have also reported the use of the reaction between sulfonamide and sulfonyl fluoride to form chemical cross-links in PFSA. The main difference in this study was the polymer synthesis, since rather than copolymerisation, sulfonyl fluoride form PFSA was treated with an amine to convert it into the sulfonamide form, followed by thermal treatment to induce cross-linking through sulfonimide linkages. The unreacted sulfonyl fluoride was then hydrolysed into sulfonic acids to give the cross-linked PFSA membrane. Direct identification of the cross-linking sites was achieved using X-Ray Photoelectron Spectroscopy (XPS) where the sulfonamide (SO_2—NH_2) and sulfonimide (SO_2—NH—SO_2) can be distinguished by the N1s and S2p spectra. Thermal pre-treatment prior to analysis served to adjust the ratio of sulfonamide to sulfonimide in the membrane.

Xu et al. [29] reported the synthesis of a cross-linkable fluoropolymer with the cross-linkable amine groups at the end of the polymer main chain rather than side chains, which was designed to retain the main chain structure of PFSA and ensure a continuity of proton transport channels. In this study, the cross-linking was achieved with an isocyanate curing agent, forming urea linkages. The cross-linked membrane shows lower water uptake and proton conductivity than non-crosslinked membrane, and also greatly reduced methanol permeability. Smaller hydrophilic domains were visible in Transmission Electron Microscopy (TEM) images of the crosslinked membrane, with domain size of 2–3 nm in contrast to 5–6 nm for Nafion, which in turn gave rise to smaller conduction channels, so restricting the flow of larger molecules such as methanol.

A different approach was presented by Greso et al. [30], who reacted the sulfonyl fluoride form of Nafion® with 3-aminopropyltriethoxysilane (APrTEOS). FT-IR analysis shows the presence of sulfonamide linkages, and the condensation of SiOR groups provided cross-linking through a covalently bound inorganic phase in the polymer. This method relies on diffusion of AprTEOS, and a membrane was obtained with a highly crosslinked outer layer and a lightly crosslinked centre, which manifested as a highly vermiculated surface in the optical and Scanning Electron Microscopy (SEM) images.

Sauguet et al. [31] have synthesised cross-linkable partially fluorinated copolymers containing alkyl bromide functionalities. The polymer was prepared by radical terpolymerisation of vinylidene fluoride (VDF) with 8-bromo-perfluorooct-1-ene (BDFO) and perfluoro(4-methyl-3,6-dioxaoct-7-ene) sulfonyl fluoride (PFSVE) to create a terpolymer with both brominated and sulfonated side chains. The bromine functionalities were then cross-linked by heat treatment in the presence of stoichiometric quantity of a peroxide and triallyl isocyanurate to obtain a film that is insoluble in organic solvents. In order to prevent side reactions through the sulfonyl fluoride, the terpolymer was first hydrolysed and thus was cross-linked in its Li salt form.

In the patent literature, Hamrock et al. [32] have claimed various methods on the chemical cross-linking of PFSAs, on works based on the short-side chain 3M ionomer. Several types of cross-linking groups were investigated, including sulfonimides [33], sulfones [34], and nitrile trimerisation [35]. To form sulfonimide linkages, PFSAs containing sulfonamide pendant groups were reacted with a sulfonyl halide group on either a side chain functionality or an aromatic moiety. The use of aromatic sulfonyl halide resulted in several interesting possibilities, as in addition to cross-linking the aromatic moiety can be further sulfonated to provide multiple acidic sites on a single sulfonimide side chain.

Another method claimed by the same group involves cross-linking by sulfone linkages [34]. PFSAs with a second, alkyl halide pendant group (Cl, Br, or I) were synthesised, which can be cross-linked with sulfonyl fluoride groups by electron beam irradiation. They also claimed the possibility of cross-linking through nitrile trimerisation of cyanide pendant groups.

Gao et al. [36] also utilised pendant alkyl bromide group as the crosslinking site, which was obtained through the copolymerisation of fluorinated monomers containing either a sulfonyl fluoride or an alkyl bromide pendant group. The resultant Br-containing PFSA can be cross-linked by heat treatment, and show reduced dimensional change upon swelling and higher elastic modulus (Fig. 3).

Plasma-induced grafting has also been used to create a cross-linked surface layer on Nafion®. Bae et al. [37] grafted styrene and

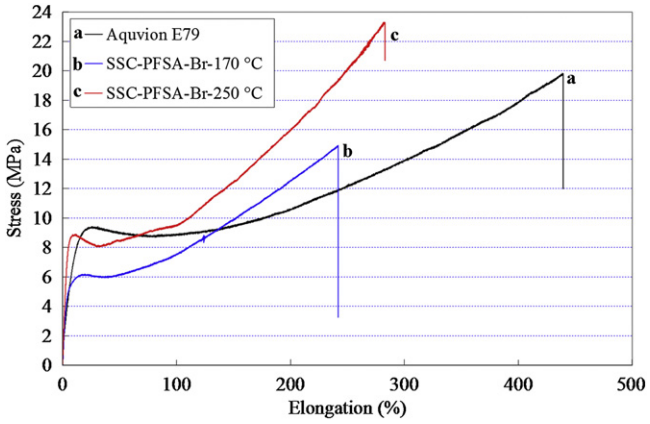

Fig. 3. Stress-strain curves of 30 μm thickness membranes of Aquivion E79 and cross-linked SSC-PFSA-Br cured at 170 °C and 250 °C [36].

divinyl benzene onto Nafion® 117, which were then sulfonated to create a layer of crosslinked poly(styrenesulfonic acid) on the membrane. However, this study was aimed at reducing methanol crossover, and the plasma-induced polymerisation was only capable of creating a barrier layer rather than cross-linking of the bulk membrane, and thus it only affects the Nafion® surface with the bulk membrane remaining unmodified.

3.2. Chemical stabilisation of PEM

Since the mechanical integrity is greatly affected by the degradation of the polymer, use of chemical stabilisation methods that mitigate polymer degradation is also a viable approach to improving the mechanical properties (and hence the long-term durability) of proton exchange membranes. Curtin et al. [38] suggested that the primary degradation mechanism of PFSA membranes takes place through radical attack on residual H-containing terminal bonds, and proposed stability enhancement by fluorination of these unstable terminal groups [39]. The stabilised membrane shows a doubling of the lifetime despite showing similar tensile strength and puncture resistance to untreated Nafion®.

Another approach focuses on minimizing the effect of reactive oxygen species through the use of peroxide-decomposition catalysts or free radical scavengers. This approach mitigates chemical degradation of the membrane by reducing the hydroxyl radicals, preventing the 'unzipping' reaction responsible for PFSA degradation [11,40], thus resulting in greater mechanical stability over time. Studies by Ramani et al. [41–43] have explored the use of various membrane additives including metal nanoparticles, metal oxides, and heteropolyacids (HPA). It was reported that platinum group metals lowered the Fluoride Emission Rate (FER) in accelerated ageing testing, and that these metal acted as free radical scavengers. The reduction in FER was greatest with gold nanoparticles, and lowest with silver, which was attributed to their relative propensity to dissolve within the PEM (their relative ease in producing metal ions). However, their protective effect was significantly lowered when the nanoparticles were anchored to an inorganic support such as silica.

Several patents [44–47] exists on the use of chemical additives such as metal salts and organometallic compounds, particularly salts and oxides of Ce and Mn, as radical quenchers to improve membrane stability. Endoh et al. [48,49] and Coms et al. [50,51] reported the use of such cationic radical quenchers incorporated into the membrane through ion-exchange. They found that Ce^{3+} and Mn^{2+} salts are especially effective in protecting PFSA membranes against decomposition by hydroxyl radicals, even at low loadings. MEAs made using the stabilised membranes show greatly reduced fluoride emission rate and little degradation after 4000 h of operation, with the decrease of MEA performance being attributed to cathode degradation rather than membrane degradation. Ce^{3+} was also shown to be four times more effective than Mn^{2+} at mitigating fluoride emission as well as more advantageous in reducing OCV decay.

Similarly, the use of HPAs as peroxide decomposition catalysts have been investigated. Haugen et al. [52] found that the protective effect of the HPA depends significantly on the stability of said HPA, with the more stable HPAs halving the rate of fluoride emission during accelerated lifetime testing. Ramani et al. [41] proposed that the stability of such membranes can be further improved by substituting the protons in the HPA with large cations to limit the solubility and thus leaching of the HPA additive. Xiao et al. studied [53] the use of zirconia as peroxide degradation catalyst and found that the presence of ZrO_2 nanoparticles reduced the OCV decay rate and the FER by an order of magnitude, which was comparable to the aforementioned results obtained with the metal nanoparticles.

Interestingly, Danilczuk et al. [54] also reported that short-side chain 3M® and Aquivion™ PFSA also show greater stability to attack by hydroxyl radicals than Nafion® which was attributed to the absence of the second ether group and the tertiary carbon in the side chains, which suggests that in the short-side chain PFSAs, radical attack occurs principally on the carboxylic end groups and the side chains themselves are not subject to significant radical attack.

3.3. Thermal stabilisation of PEM

It is known that heat treatments can improve the mechanical stability of polymeric materials through the increase in the degree of crystallinity of the polymer and the reduction of the free volume between polymeric chains. Therefore, heat treatments can be used to achieve physical stabilisation of ionomeric membranes. Membrane reconstruction of Nafion from high-boiling point solvents results in a reduced solubility and better mechanical properties [55]. Moreover, the annealing of recast Nafion 1100 membranes in the temperature range 150–250 °C induces strong modification of the diffraction pattern during the first heating hour, while thermal treatments over 3 h have only little effect [56]. More specifically, the wide-angle X-ray patterns of the annealed samples reveal the progressive sharpening of the Bragg peak centred around $2\theta \sim 21^{\circ}$ as temperature increases. The structural modifications induced by the annealing are confirmed by small angle X-ray spectra showing that crystalline order, characterised by a longer repetition distance, develops with increasing temperature.

4. Polymer-reinforced PFSA membranes

Currently, the most mature technology in reinforced PFSA membranes is that of PFSA reinforced with a mechanically stable polymer matrix, of which there are many studies and also several commercially available products. A majority of these utilise poly(-tetrafluoroethylene) (PTFE) [57–65] due to its excellent stability and mechanical strength. Such composite membranes possess several advantages in mechanical properties compared to non-modified membranes, such as an increase in their mechanical strength and better dimensional stability upon swelling. The improved mechanical properties allow the fabrication of very thin membranes, the use of which is expected to improve water management during PEMFC operation [66] and further reduce the material cost. However, the main motivation for developing thinner membranes is to lower the internal resistance, as the reduction in area resistance with decreasing thickness is substantial. The challenge in developing thinner membranes is achieving the required mechanical strength and durability especially at elevated temperatures and in the presence of water.

Currently, several different types of inert reinforcement have been developed by various groups, such as porous expanded PTFE (ePTFE) sheet (from W.L. Gore [67] and other authors [68–70]) or micro PTFE fibril (from Asashi Glass Co. [71]), porous polypropylene [72], poly(vinylidene fluoride) (PVdF) [73], and polysulfone/microglass fibre fleece [74]. Other studies used PTFE reinforcement with non-PFSA polymer electrolyte filler, including sulfonated polystyrene [75] and sulfonated poly(ether ether ketone) [76]. In some of these reinforced membranes, the membrane thickness can be reduced to 5–30 μm while retaining sufficient proton conductivity and mechanical properties [77,78]. In such thin membranes, the back diffusion of water from the cathode to the anode in the cell is more effective, in particular when using reduced dew point reactants.

4.1. PFSA membranes reinforced with PTFE

Early developments of reinforced PFSA membranes aimed at chlor-alkali electrolysis applications used woven PTFE fabrics as a standard reinforcement because of their good mechanical strength and stability [79]. However, this application uses membranes of significant thickness (200–300 μm) whereas in PEMFC applications, a thin and flat membrane is required to obtain good cell performance. To overcome this issue, Penner and Martin [61] used expanded, porous PTFE (ePTFE, Gore-Tex) membrane rather than woven PTFE fabric as a reinforcement for PFSA membranes, which became the basis of the Gore-Select membrane. Due to the presence of inert, non-conductive reinforcement, such reinforced membranes generally show reduced proton conductivity compared to the corresponding non-reinforced PFSA. In the case of ePTFE reinforced membranes, the conductivity loss is disproportionately greater than what would be expected based on the PTFE volume fraction [80]. This has been attributed to the inherent incompatibility of the inert, low dielectric PTFE and the highly ionic PFSA leading to a collapse of the ePTFE layer during membrane fabrication, resulting in a PFSA-deficient layer which can be seen on the SEM EDX analysis of sulfur content in the membrane cross section (Fig. 4). This deficiency also results in the PFSA-deficient region drying out under reduced hydration, limiting the membrane conductivity at low RH.

However, despite the lowered conductivity, their improved mechanical properties [81,82] meant that thinner membranes (5–30 μm) can be used compared to 50–200 μm for non-reinforced PFSA membranes, significantly reducing their area resistance. Furthermore, concurrent developments in the field such as lower Equivalent Weight (EW) PFSAs can be expected to help counterbalance the reduction in proton conductivity and obtain improvements in both fuel cell performance and lifetime.

Other developments have also followed, such as that by Bahar et al. [59] who used surfactant to ensure complete impregnation of the matrix, Tang et al. [83] who improved the durability of Nafion®/PTFE membranes by high-temperature thermal treatment, the study by Liu et al. [84] of Nafion®/PTFE composite membranes using several types of porous PTFE films, and Tang et al. [85] who used a hydrophilically modified expanded PTFE matrix to increase the PFSA resin loading. Although the hydraulic permeability of composite membranes is dramatically increased [86] due to their significantly reduced membrane thickness and to the hydrophobicity of PTFE, the composite membranes generally show a lower water content at a given temperature compared to pure Nafion® as the porous PTFE suppresses volumetric swelling.

This also means that the dimensional stability of the membrane depends on the PTFE content, with thinner composite membranes (higher relative PTFE content) providing better dimensional stability than thicker ones. Similarly, increasing the pore size of the reinforcing matrix results in increased proton conductivity (and hence cell performance) but also increases water uptake and reduces dimensional stability [87]. In contrast, oxygen permeability coefficients of composite membranes at a given temperature were slightly larger than those of Nafion® membrane, which was attributed to presence of PTFE in the composite membranes, which makes them more hydrophobic than Nafion®, as it was postulated that the oxygen diffuses through the hydrophobic domains.

The increased dimensional stability and better resistance to tear propagation of composite membranes translate to significantly higher durability in a PEMFC stack. Physical leak test and OCV decay rate of a composite membrane correspond to a six-fold increase in lifetime compared to non-reinforced membranes, with membrane failure coming from chemical attack on the PFSA which results in removal of ionomer from the support structure rather than through the breaking or fracturing of the membrane perpendicular to the catalyst layer observed in non-reinforced membranes (Fig. 5). In this regard, it is also important to achieve full impregnation of the PTFE matrix, as defects such as voids or pinholes may become weak points in the PEM susceptible to hydration-induced stresses.

However, mechanical reinforcement alone may be insufficient to prevent mechanical failure from wet/dry humidity cycling, and casting conditions also play a very significant role in terms of membrane durability [79]. Tang et al. [70,85] have studied the use of surfactants or a chemically modified PTFE matrix in order to ensure better penetration of the Nafion® solution into the porous PTFE matrix. This improves the PFSA loading of the composite membrane and also betters the resistance to hydrogen crossover under an accelerated wet/dry cycling test.

It should also be noted that in addition to pore filling, there is also a need for a continuous thin film of Nafion® on the PTFE surface as this is necessary for the preparation of the MEA, as during MEA fabrication (hot-pressing) this surface film of Nafion® is required for good adhesion with the electrodes. Thus, SEM images of the surface of composite membranes generally show a smooth surface, with the presence of the reinforcing matrix visible only in the cross section (Fig. 6).

Most PTFE/PFSA composite membranes are prepared by impregnation of an expanded PTFE matrix by a PFSA solution, but variations of the impregnation method have been described by Ahn et al. [88] and also in a patent by Toyota [89] which fabricates reinforced membranes using a molten electrolyte resin in the sulfonyl fluoride form rather than a PFSA polymer solution. The molten perfluorosulfonyl fluoride resin has the advantage of being less hydrophilic than PFSA and thus can be easily impregnated into the hydrophobic PTFE support. The two fabrication approaches differ in their impregnation method, as Ahn et al. [88] created their reinforced composite membrane by placing perfluorosulfonyl fluoride resin films on either side of an expanded PTFE film followed by

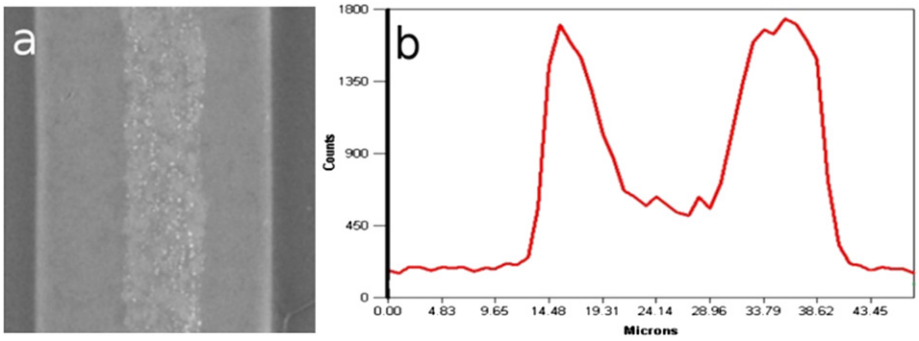

Fig. 4. Cross-section SEM (a) and sulfur EDX (b) analysis of ePTFE-reinforced PFSA membrane [80]. S. Banerjee, D. Prugh, S. Frisk, *ECS Trans*., 50 (2012) 887-895. Reproduced with permission from The Electrochemical Society.

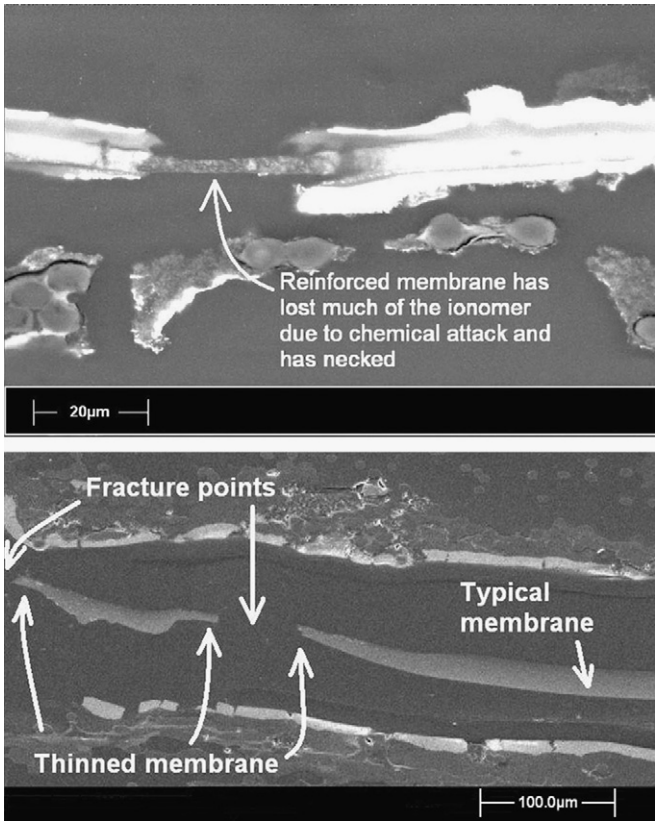

Fig. 5. Post-mortem SEM images on MEAs using reinforced (top) and a non-reinforced (bottom) PFSA membrane [68]. T.R. Ralph, D.E. Barnwell, P.J. Bouwman, A.J. Hodgkinson, M.I. Petch, M. Pollington, *J. Electrochem. Soc.*, 155 (2008) B411-B422. Reproduced with permission from The Electrochemical Society.

hot-pressing at 240 °C and 10 atm, whereas Toyota has developed a method whereby the molten resin is discharged from a die and a porous reinforced membrane is embedded into the extruded molten electrolyte resin by two heated rotating rolls arranged opposite to each other.

Asahi Glass Company [90,91] developed composite membranes reinforced with PTFE fibrils. The composite membrane contains PTFE-fibrils of submicron diameter which are uniformly dispersed within the ion-exchange membranes. When their properties such as tensile strength, tear strength, creep and compressive properties were examined and compared with those of non-reinforced membranes, they show that even the addition of a small amount of PTFE-fibrils (2.7 wt.%) improves their mechanical properties especially the tear strength which was 6–18 times larger than those of the other non-reinforced membranes. This improvement is however anisotropic (different tear strength in the machine and transverse direction) due to the orientation of the PTFE fibrils. In a fuel cell, the performance of the reinforced membrane is nearly equal to non-reinforced ones and cell voltage remained around the same value during 3000 h of cell operation at 80 °C, indicating good long term durability. By limiting the quantity of PTFE fibrils to a small amount, the hydrogen permeability coefficients and AC specific resistance of the reinforced membrane were kept to similar values to other PFSA membranes.

More recently, secondary additives in PTFE reinforced membranes have been investigated to further improve their performance, using substrates such as zirconium phosphate [92], and Pt nanoparticles [93]. Nafion®/PTFE composite membranes containing ZrP (NF-ZrP) have been prepared via two processes. In a first, a submicron porous PTFE membrane was impregnated directly in a Nafion®/$ZrOCl_2$ solution (NF–Zr-d). In a second method, submicron porous PTFE membrane was impregnated in a Nafion® solution to prepare the NF composite membrane, which was then impregnated in a $ZrOCl_2$ aqueous solution via a so-called in situ precipitation method (NF–Zr–I). Incorporating silicate and zirconium phosphate into NF membranes enhances water retention of membranes at temperatures above 110 °C and improves PEMFC performances [94,95].

Liu et al. [93] described a poly(tetrafluoroethylene) (PTFE)/Nafion® composite membrane with self-humidifying ability utilising highly dispersed Pt nanoparticles through a poly-diallyldimethylammonium chloride (PDDA)-stabilization method which was earlier published by Tian et al. [96]. To fabricate the membrane, they immersed a pre-treated porous PTFE film in a solution of Pt-PDDA to allow the nanoparticles to attach within the pores via electrostatic interaction, followed by pore-filling with Nafion®. The Pt nanoparticles suppress reactant crossover and generate water through catalytic recombination of the reactant gases, without the risk of Pt aggregation and short circuit as the Pt nanoparticles are fixed onto the walls of the porous PTFE matrix, resulting in the composite membrane showing better performance than PTFE/Nafion® membrane under dry conditions.

4.2. PFSA membranes reinforced with other polymers

Other inert polymers have also been used as matrices for composite Nafion® membranes, although these studies have generally been geared towards DMFC applications, where the main interest lies more towards reducing methanol crossover rather than mechanical reinforcement. Nguyen et al. [97] reported the fabrication of a composite membrane of Nafion® reinforced with a highly porous polyimide (PI) film. This film was fabricated by a wet phase inversion technique using a solvent/non-solvent mixture of DMF

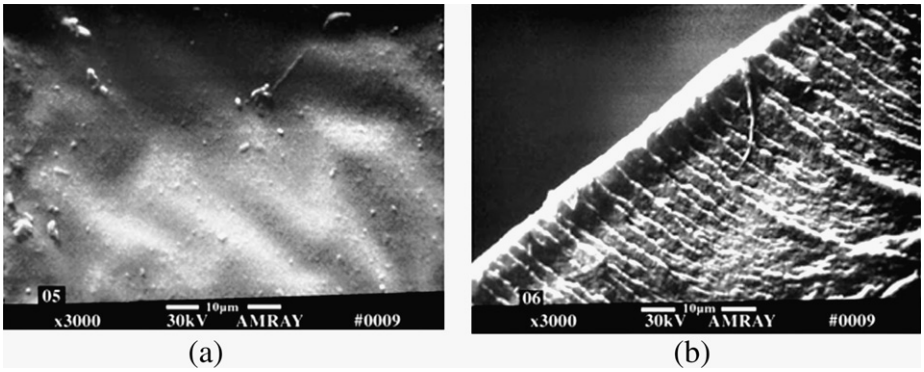

Fig. 6. SEM images of (a) surface of Nafion®/PTFE composite membrane and (b) cross-section of the composite membrane [84]. Reprinted from *Journal of Membrane Science*, Vol 212, Issues 1-2, F. Liu, B. Yi, D. Xing, J. Yu, H. Zhang, Nafion/PTFE composite membranes for fuel cell applications, Pages 213-223, Copyright (2003), with permission from Elsevier.

and 1-butanol, the ratio of which determines the porosity of the resultant film. It was found that a 'wet' porous polyimide film with residual acetic anhydride (from the PI synthesis) was necessary to ensure complete impregnation of the porous matrix, as completely dry PI does not possess sufficient wettability even when post-treated with acetic anhydride.

Yildirim et al. [98] used microporous Ultra-High Molecular Weight PolyEthylene (UHMWPE, Solupor) film as a reinforcing matrix, and reported that the lower methanol crossover was sufficient to compensate for the reduced proton conductivity, leading to better DMFC performance. However, the cross section of their membrane indicates that the pores of the UHMWPE are not completely filled, with a porosity of 27% after impregnation (the porosity of the pristine UHMWPE film was 85%).

A similar approach was used by Shim et al. [99], who utilised a 6 μm film of hydrophilic polyethylene terephthalate (PET) as a reinforcement for Nafion®, and also deposited a very thin film of palladium (20 nm) on the anode side of the membrane. In addition to the PET reinforcement, the palladium film greatly reduced methanol crossover, with higher current density at given cell voltage in DMFC operation compared to Nafion® 117.

Rather than a porous matrix, Pu et al. [100] utilised a semi-interpenetrating polymer network (semi-IPN) of polyvinylidene fluoride [101] or fluorine-containing polyimide [102]. In this approach, Nafion® is blended with the reinforcing polymer which, in the case of the polyimide, contains cross-linkable functionalities such as carboxylic acid or vinyl groups, whereas the polyvinylidene fluoride was cross-linked by electron beam irradiation. The cross-linked IPN significantly improves the tensile strength and reduced the swelling of Nafion®, however the presence of non-conductive filler resulted in reduced proton conductivity, with the drop in proton conductivity depending more on the filler content rather than on the degree of cross-linking.

4.3. PFSA membranes reinforced with an electrospun matrix

Recently, porous nanofibre mats made by electrospinning [103] have been utilised as mechanical reinforcement for PFSA membranes [104]. Unlike conventional fibre production method such as extrusion, electrospinning uses an applied potential difference between a polymer solution (in a syringe) and a grounded collector to form long strands of nanofibres, resulting in the deposition of a highly uniform, nonwoven porous mat on the collector surface. Such nanofibre matrices have the advantage of better interconnectivity and uniformity compared to those prepared by conventional methods such as phase inversion, with greater versatility during fabrication through the control of the electrospinning parameters.

In this approach, an inert or sulfonated hydrocarbon polymer is electrospun into a porous mat which is then impregnated with a PFSA solution. Since the proton conductivity of the membrane depends mostly on PFSA content, the conductivity of such composite membranes is generally lower than that of pure PFSA, however other properties which may be significant (in addition to mechanical properties) such as barrier properties and methanol permeability can be significantly improved. Indeed, studies such as by Choi et al. [105] who utilised electrospun poly(vinylidene fluoride) (PVdF) as a reinforcing matrix found significant reduction in proton conductivity of an order of magnitude compared to Nafion® 115 due to the presence of PVdF. In their study, the main advantage of the composite membrane was in reducing methanol crossover, and thus the composite membrane showed comparable performance to Nafion® in a DMFC application.

Molla et al. [106,107] have investigated the use of electrospun poly(vinyl alcohol) (PVA) matrix, which was cross-linked by a treatment with glutaraldehyde. Repeated impregnation steps and hot pressing were used to ensure a thorough impregnation of the PVA, which resulted in only a slightly lowered proton conductivity compared to Nafion®, while achieving good mechanical properties for membranes that are 20–60 μm thick. Here too, the intended application of this membrane was for DMFC, for which the PVA composite shows comparable results to Nafion® of similar thickness. The Nafion®-PVA system has also been studied by Lin et al. [108], who found that the use of a porous, electrospun matrix allows greater percentage of PVA to be used compared to blend membranes, as the electrospun PVA-Nafion® membranes (containing 10% PVA) shows the same DMFC performance to values reported in a previous study on Nafion®-PVA blend membranes [109] that has an optimum PVA content of 5%.

Since the use of an inert polymer matrix results in a reduction of proton conductivity, Shabani et al. [110,111] have tried to overcome this by using a sulfonated or partially sulfonated poly(ether sulfone) as the electrospun matrix polymer. The composite membranes showed comparable proton conductivity to Nafion®, but with reduced methanol permeability. In these studies an excess of Nafion® was cast on one or both sides of the membrane to form a bi- or triple-layer membrane. Although there were no significant differences in the performance between them, it should be noted that in the case of the bilayer membrane better results (in DMFC testing) were obtained with an alternative fabrication method where the SPES was electrospun directly onto Nafion 112 membranes followed by impregnation and pore filling (rather than by casting an extra layer of Nafion® dispersion on top of the pore-filled membrane). This may be due to better crystallinity in commercial Nafion® compared to Nafion® cast from dispersion (which was only annealed at 120 °C in their study), but these differences in the performance of the bilayer membrane were also smaller relative to the difference between the composite membranes and Nafion® 112 or 117 alone. Hwang et al. [112] also reported the fabrication of electrospun SPES impregnated with Nafion®, and similarly observed reduced methanol crossover.

Lee et al. [113] used an electrospun polyetherimide (PEI) matrix as a reinforcement for Nafion® membranes. In order to improve solution penetration during impregnation, they coated the PEI with hygroscopic SiO_2 nanoparticles. Although the silica reduces the porosity of the matrix from 90% to 70%, it also improves the tensile modulus (from 0.77 to 1.96 MPa) and greatly improves the wettability of the PEI matrix. Furthermore, it also improves the adhesion between the Nafion and the PEI matrix and slows down the rate of water loss at high temperatures due to the presence of chemically adsorbed water on the surface of the silica nanoparticles.

An alternative approach is to fabricate a porous PFSA nanofibre matrix which can then be reinforced by other polymers. Porous nanofibres of Nafion® [114,115] and other PFSAs [116,117] have been successfully fabricated by electrospinning, and combining such fibres with a more mechanically stable polymer can provide a mechanically reinforced membrane. Although most studies in this area have only gone as far as electrospinning the PFSA nanofibres, studies by Pintauro et al. [116,118] have shown that such an approach (utilising a UV-curable polyurethane resin as reinforcing polymer) with Nafion® or 3M PFSA allows for lower dimensional swelling and improved mechanical properties compared to cast membranes.

5. PFSA mechanical reinforcement by inorganic fillers

The incorporation (preferably on a nanometric scale) of a solid filler into the polymer matrix can significantly improve the mechanical properties of PFSA membranes [119]. In this type of (nano) composite system, the filler may interact either with the hydrophobic polymer backbone or with the sulfonic functional groups, and the filler – polymer interaction can range from strong (covalent, ionic) bonds to weak physical interaction.

Besides the mechanical properties, there are several membrane properties that may benefit from the presence of uniformly dispersed fillers, such as reduced permeation of reaction gases and radical species that could contribute to oxidative degradation, reduced swelling, enhanced water management, as well as an enhancement in proton conductivity if the filler possesses significant concentration of protonic groups. There are many types of fillers used for the mechanical stabilisation of PFSA membranes, including carbon nanotubes, oxides and layered materials, such clays and zirconium phosphate. Each of these materials possess their own advantages and challenges, as will be discussed below.

5.1. Nanotubes

Carbon nanotubes (CNTs) are a new class of advanced filler materials with very interesting properties and capacity for improving the mechanical properties of polymer matrices. Until very recently, their use as a filler within fuel cell membranes was not considered mainly because of the risk of a short-circuit caused by a non-electronically isolated electrolyte. In 2006, Liu et al. [120] demonstrated that this problem could be solved by keeping the content of CNTs lower than the percolation threshold (Fig. 7). The mechanical stability of Nafion membranes was improved by dispersing 1 wt% CNTs, without affecting the performances of the H_2/O_2 fuel cell: the strength of the composite Nafion® – 1 wt% CNT membranes increased by about 69 and 29% compared with that of recast Nafion® and Nafion® NRE-212, respectively. However, the method used for the dispersion of CNTs – a ball-milling method followed by solvent casting – may not be appropriate for scaling-up.

Wang et al. [121] reported an improved solution-cast method to prepare Nafion®/Multi-Walled CNT (MWCNT)-reinforced membranes with MWCNT content from 1 to 4 wt.%. MWCNTs were oxidized by H_2O_2 and sodium hydroxide was added into the MWCNT/Nafion®/N,N-dimethylacetamide solution. Scanning electron microscopy showed that the MWCNTs were uniformly dispersed in the Nafion matrix. The tensile strength and the elongation at break were greatly improved for the reinforced membranes compared to the recast Nafion membranes (54 and 27%, respectively). The fuel cell performance of the reinforced membranes with different MWCNTs contents was also tested at 80 °C under fully humidified conditions. By comparing mechanical properties, proton conductivity and fuel cell performance of the reinforced membranes, it can be concluded that the content of MWCNTs in the reinforced membranes should not exceed 3 wt%. The MWCNTs/Nafion® reinforced membrane with 3 wt% MWCNTs content showed the best mechanical characteristics and excellent fuel cell performance.

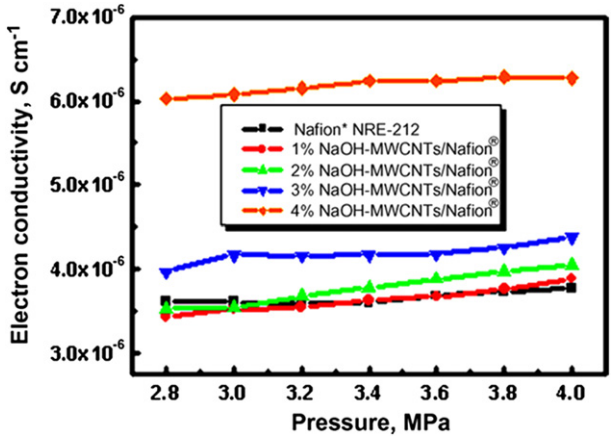

Fig. 7. Electronic conductivity of Nafion/MWCNT composites [121]. Reprinted from *Journal of Power Sources*, Vol 176, Issue 1, L. Wang, D.M. Xing, H.M. Zhang, H.M. Yu, Y.H. Liu, B.L. Yi, MWCNTs reinforced Nafion membrane prepared by a novel solution-cast method for PEMFC, Pages 270-275, Copyright (2008), with permission from Elsevier.

Thomassin et al. [122] prepared MWCNTs-based Nafion® membrane by a melt-extrusion method in order to decrease the MeOH permeability without deleterious effect on the ionic conductivity. For the preparation of composites, two different types of MWCNTs were used: neat MWCNTs and MWCNTs functionalised by carboxylic acid (MWCNT–COOH). The effect of the MWCNTs on the mechanical properties of the Nafion® membranes was evaluated by tensile testing at room temperature. The Young's modulus was increased by 140% and 160% for MWCNT contents of 1 and 2 wt% respectively as compared to pure Nafion®. The increase in the Young's modulus was slightly higher in case of MWCNT–COOH, consistent with better filler dispersion. In each case, the Young's modulus levels off at MWCNT contents exceeding 2 wt%, in relation to the incipient aggregation of the nanotubes. No electronic conductivity was measured for nanofiller content lower than 2 wt%, so that any risk of short-circuit was avoided. On the other hand, the methanol permeability was significantly decreased whereas only a slight decrease in the ionic conductivity was observed.

More recently, further work was carried out to investigate the effect of CNTs surface functionalisation on the thermo-mechanical stability of CNTs-based composite membranes [123]. Nafion® membranes containing 1 wt% carbon nanotubes were prepared via melt-blending at 250 °C using three different types of CNTs: pure CNTs (pCNTs), oxidised CNTs (oCNTs) and amine functionalised CNTs (fCNTs). These membranes, as well as non-modified Nafion®, were characterised by DMA tests in the temperature range 25–180 °C. In all cases the tan δ curves show only one peak attributed to the glass transition. For the pristine Nafion® membrane the glass transition appears at about 140 °C and shifts to higher temperature when pCNTs and oCNTs are incorporated into the Nafion® matrix. The highest glass transition temperature ($T_g \sim 160$ °C) is observed for the composite membrane containing oCNTs. This marked improvement in thermo-mechanical stability is due to the homogeneous dispersion of o-CNTs in the Nafion® matrix, as a result of the possible strong interaction between the COOH groups on oCNTs outer surfaces and sulfonic groups of the Nafion® matrix. However, in the case of composite membranes loaded with fCNTs, the T_g of matrix shifts to about 125 °C, indicating poorer thermo-mechanical stability which is associated with the poor dispersion of fCNTs in the Nafion® matrix.

5.2. Oxides

Binary metal oxides have been widely used as fillers of PFSA membranes not only to enhance their mechanical properties but also to improve the membrane water retention so as to enable better fuel cell performance at higher temperature (i.e. above 80 °C) and/or at low relative humidity (e.g. working with low dew point feed gas). On the other hand, only very few papers report the use of organically modified oxides as hydrophobic fillers, purposely designed to interact with the perfluorinated PFSA backbone.

From the synthetic point of view, PFSA/metal oxide composite membranes are prepared according to two main synthetic approaches: one is based on the casting of dispersions of the preformed oxide in the PFSA solution, while the second consists in the in situ growth of an oxide within the preformed PFSA matrix. Therefore this section is divided in three subsections dealing with composites loaded with *i*) in situ grown oxides, *ii*) preformed oxides and *iii*) organically modified hydrophobic oxides.

5.2.1. In situ grown oxides

Nafion–SiO_2, Nafion®-dimethylsiloxane and Nafion–ORMOSIL hybrids [124] were created via in situ sol–gel copolymerisation of tetraethoxysilane (TEOS), diethoxydimethylsilane (DEDMS), and their mixtures, leading to the formation of two types of structural units in the copolymer: *Q* unit (i.e. $Si(O_{½})_4$) and *D* unit (i.e. $(O_{½})_2Si(CH_3)_2$). Subsequently, semiorganic comonomers other than DEDMS were also employed in the generation of Nafion/ORMOSIL hybrids with TEOS/semiorganic comonomer molar ratios of 1/0, 2/1, 1/1, 1/2, 0/1 [125]. Specifically, TEOS–triethoxyvinylsilane, TEOS–methyltriethoxysilane, TEOS–phenyltriethoxysilane, TEOS–diethoxymethylvinylsilane and TEOS–hydroquinone combinations were used. DMA analysis carried out on unfilled Nafion® and on the hybrids showed in all cases a higher temperature of the α-transition (T_α) for the hybrids that was attributed to immobilization of the Nafion® side chains by their entrapment in silicon oxide domains. Moreover, the transition temperature of the pure silicate-filled hybrid was considerably higher than that of any other hybrid, presumably because of the rigidity of silicate structures. Some, but not all, of the ORMOSIL combinations display trends in transistion temperature with respect to the TEOS/comonomer ratio. The most organized trend is that for TEOS/DEDMS-modified Nafion®: the Q:D progression 0:1 → 1:2 → 1:1 → 2:1 → 1:0 displays increasing mechanical tensile strength and decreasing ductility, which is rationalized in terms of decreasing flexibility of the ORMOSIL nanostructures.

In situ sol–gel polymerisation of titanium isopropoxide was also used to generate titania quasi-networks in the polar domains of Nafion® with the aim of improving the membrane durability [126]. The incorporated titania reduced water uptake without significant change of the equivalent weight. Mechanical analysis of contractile stress, buildup during drying from a swollen state in samples clamped at constant length, demonstrated considerable reinforcement of Nafion® by the titania structures. Tensile studies showed that at 80 °C and 100% relative humidity the dimensional change of the composite membrane is one half and the elastic modulus is three times higher in comparison with that of the unmodified membrane. Fuel cell performance of the composite membrane was inferior to that of the unfilled Nafion® membrane. However, during an open circuit voltage decay test, the composite membrane showed lower voltage decay rate (by 3.5 times) and strongly reduced fluoride emission (by an order of magnitude) thus indicating reduced chemical degradation. This was attributed to better gas barrier properties resulting from tortuosity introduced by the filler: a lower fuel crossover may reduce the rate of hydrogen peroxide formation and, consequently, the rate of membrane chemical degradation. These model studies indicate that this type of in situ inorganic modification offers a way to enhance fuel cell membrane durability by reducing both physical and chemical degradation.

5.2.2. Preformed oxides

Composite Nafion®/SiO_2 films, containing up to 15 wt% filler, were prepared by a solution casting procedure, using a dispersion of fumed silica nanopowders in a 5 wt% Nafion® solution [127]. DMA studies allowed to measure two mechanical relaxation modes at about 19 and 100 °C. The relaxation detected around 100 °C is attributed to the motion of clusters of side chains and is diagnostic for $R–SO_3H\cdots SiO_2$ nanocluster interactions. The results of DMA tests showed that, at $SiO_2/–SO_3H$ molar ratios lower than 1.9, the filler particles restrict chain mobility of hydrophobic domains of Nafion® and the dynamics inside polar $–SO_3H\cdots SiO_2$ clusters; however, at higher molar ratios, the filler particles reduce the cohesiveness of hydrophilic polar domains. Neutralization of Nafion®/SiO_2 by triethylamine (TEA) increases the storage modulus at room temperature due to the formation of $R–SO_3^-\cdots HTEA^+\cdots SiO_2$ bridges [128].

Fumed silica was also used to prepare Nafion® based nanocomposite membranes, by solution casting, in the presence of an anionic fluorosurfactant (Zonyl TBS) [129]. This surfactant, which contains a sulfonic acid group, facilitates the dispersion of the silica nanoparticles and simultaneously enhances the proton conductivity. Mechanical tests were carried out on Nafion–silica nanocomposite membranes with and without fluorosurfactants, as well as on a neat Nafion®-recast membrane, by stretching the membranes in both dry and wet states. All wet membrane samples had lower mechanical strength than dry samples, and the Nafion®–silica nanocomposite membrane had a lower tensile strength than the Nafion®-recast membrane. The incorporation of fluorosurfactant into the Nafion®–silica nanocomposite membrane improved the mechanical properties of the membranes regardless of their states (dry or wet) in comparison with the membranes without fluorosurfactant and to the neat Nafion®-recast membrane. An MEA based on the nanocomposite Nafion®–TBS–1 wt% silica was tested at 80 °C and showed up to 61% higher current density at 0.6 V in comparison with Nafion 112 at 80 °C.

Composite Nafion® membranes with various loading of sulfonic acid functionalised hollow silica spheres (SAFHSS) were prepared by solvent casting [130] and the effects of SAFHSS on water uptake, swelling degree, mechanical properties and proton conductivity were investigated. In particular, at 25 °C and 50% RH, the Young's modulus of the composite membrane increases with the SAFHSS loading in the range 3–15 wt% up to a value about three times higher than that of pure Nafion®. Concomitantly, the tensile strength and the elongation at break decrease, being lower than those of pure Nafion® membrane. Nevertheless it was considered that the drop of these parameters is not sufficiently severe that it would significantly affect the use of the composite membranes in PEMFC.

Recast Nafion® membranes, loaded with 3 wt% TiO_2 (anatase) nanoparticles (21 nm) were investigated by mechanical tests and conductivity measurements in constrained environments so as to simulate conditions relevant to PEM fuel cell operation [131]. It was found that the elastic and plastic deformation of neat Nafion and Nafion®/TiO_2 composites decreases with both temperature and water content. In comparison with neat Nafion®, the composite membranes exhibited less strain hardening and a reduction in the long-time creep of about 40%. The inclusion of TiO_2 increased the elastic modulus and decreased the plastic modulus of Nafion® membranes, with the same trend observed under hydration (Fig. 8).

Water uptake is faster in recast Nafion® membranes in comparison with extruded Nafion® and the addition of 3% titania particles has minimal effect on the rate of water uptake. The resistivity of both neat and composite Nafion® membranes increases when the membranes are placed under a load and shows a substantial hysteresis as a function of the applied stress depending on whether the pressure is increasing or decreasing. These results show that the mechanical properties of Nafion®-based membranes will impact the dynamic performance of PEM fuel cells, especially during startup when the membranes swell as they absorb water. The results did not reveal any direct connection between the mechanical properties of composite membranes and their improved performance in PEM fuel cells.

Finally, the effect of different metal transition oxides (M_xO_y, with M = Ti, Zr, Hf, Ta, W) on the mechanical properties of recast Nafion® filled with 5 wt% oxide was investigated by DMA tests at 1 Hz [132]. At 50 °C, the storage modulus of the composite membranes is strongly dependent on the nature of the oxide metal and changes according to the sequence:

W ∼ Hf > Zr > Ti > Ta. The composite filled with tantalum oxide has about the same storage modulus as neat Nafion.

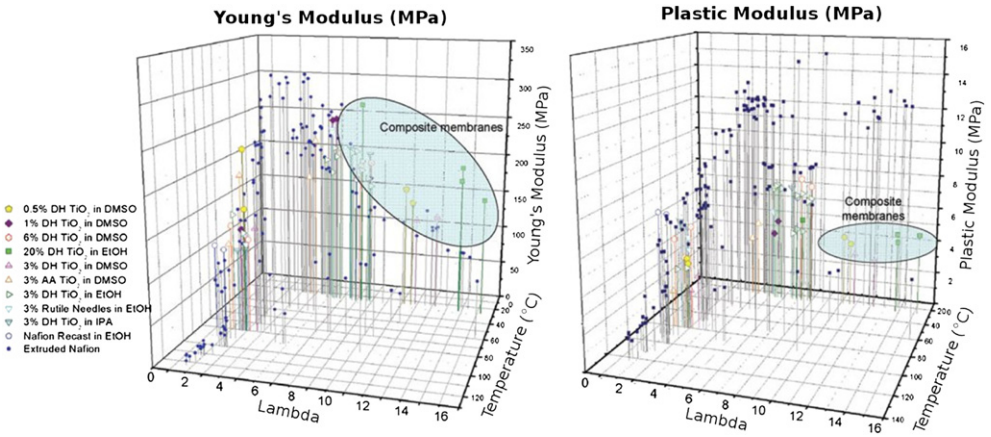

Fig. 8. Elastic/Young's modulus and plastic modulus of Nafion and Nafion/TiO2 composite membranes [131]. Reprinted from *Journal of Polymer Chemistry Part B Polymer Physics*, Vol 44, Issue 16, M.B. Satterfield, P.W. Majsztrik, H. Ota, J.B. Benziger, A.B. Bocarsly Mechanical properties of Nafion and titania/Nafion composite membranes for polymer electrolyte membrane fuel cells, Pages 2327-2345, Copyright (2006), with permission from John Wiley & Sons.

5.2.3. Organically modified hydrophobic oxides

A hydrophobic nanofiller consisting of silica "cores" bearing fluoroalkyl surface functionalities was synthesised by direct reaction between nanometre sized silica and (2,2,3,3,4,4,5,5,6,6,7,7,8,8,9,9,9-heptadecafluorononyl)oxirane. This modified silica, $Si_{80}F$, was then used to obtain a set of nanocomposite membranes with formula [Nafion/$(Si_{80}F)_x$], where x, ranging between 0 and 1.6, is the molar ratio of silicon atoms to sulfonic acid groups and corresponds to 0–10 wt% of nanofiller [133].

The mechanical properties of these nanocomposite membranes were investigated by DMA at temperatures up to 210 °C. In the range −10/50 °C the storage modulus (E′) is essentially independent of temperature. At higher temperatures E′ decreases and an irreversible elongation is observed for the neat recast Nafion membrane at 160 °C, while the [Nafion/$(Si_{80}F)_x$] nanocomposite films retain a measurable E′ up to 200 °C. All the nanocomposite membranes are stiffer than pristine Nafion, especially at high temperatures. The tan δ curves evidence an intense peak at about 100 °C that is assigned to the α relaxation, which originates in a weakening of electrostatic interactions within the ionic aggregates.

As the filler content is raised, E′ increases while the intensity of the maximum of the α relaxation peak decreases, thus indicating that a smaller fraction of the overall mechanical energy provided to the system is dispersed by this relaxation mode. This behaviour allows to conclude that the $Si_{80}F$ nanoparticles interact both with the polar domains and with the fluorocarbon hydrophobic domains of the host polymer. Indeed, the interactions between the sulfonic groups of Nafion® and residual silanol groups on the surface of the $Si_{80}F$ particles lead to an increase of E′ as x is raised. On the other hand the fluorocarbon chains on the surface of the nanofiller act as plasticizers of the hydrophobic domains of the host polymer, thus decreasing the intensity of the α relaxation peak. Therefore, with respect to pristine Nafion®, the hybrid [Nafion/$(Si_{80}F)_x$] nanocomposite films show better mechanical properties at higher temperatures. In spite of a lower water uptake in comparison with the pristine recast Nafion®, the [Nafion/$(Si_{80}F)_{0.7}$] membrane showed a significant improvement in the fuel cell performance (by about 40% with both air and pure oxygen feed) that was not affected by lowering the relative humidity down to 50%.

Nafion® membranes containing vinyl-pendant octasiloxane ($Q8M8^V$) based oligomers [134] are another example of composites filled with organically modified oxides. $Q8M8^V$ cubic molecules were included into the Nafion® matrix during the recasting process and then subjected to polymerisation so as to generate in-situ rigid poly($Q8M8^V$) nano blocks. Due to their hydrophobic nature, the filler particles interact mainly with the hydrophobic perfluorinated chains of the ionomer, rather than with the sulfonic groups, thus generating a physical cross-linking. It is also suggested that the filler plays an important role in restricting random extensions of proton-conducting channels and promotes an ordered assembling of the ionomer chains. As a consequence of the physical cross-linking, the storage modulus of the composite membranes increases with the filler loading being by 67% larger than that of pristine Nafion® for the membrane containing 15 wt% poly($Q8M8^V$). On the other hand, the increase in the storage modulus is concomitant with a shift to low temperature of the glass transition temperature (Fig. 9).

Composite membranes, with filler loading in the range 5–15 wt %, manifested improvement in lowering methanol permeability, reduction of activation energy for proton conduction and an increase in the power density output of a single direct methanol fuel cell. The best fuel cell performance, both at room temperature and 50 °C, was obtained with the membranes containing 5 and 15 wt% filler. For example, the maximum of the power density supplied by the 15 wt% membrane was 13.9 mW cm^{-2}, while that of the pristine Nafion membrane was 4.6 mW cm^{-2}.

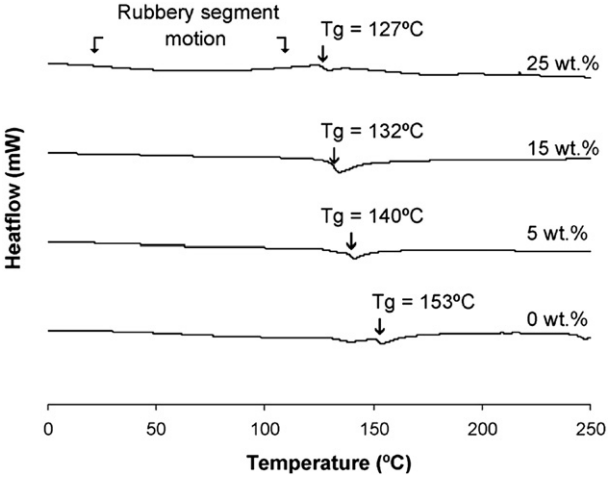

Fig. 9. DSC of recast Nafion filled with vinyl-pendant octasiloxane oligomers showing the decrease in T_g with increasing the filler content [134]. Reprinted from Journal of Membrane Science, Vol 320, Issues 1-2, X. Zhang, S.W. Tay, L. Hong, Z. Liu, In situ implantation of PolyPOSS blocks in Nafion® matrix to promote its performance in direct methanol fuel cell, Pages 310-318, Copyright (2008), with permission from Elsevier.

5.3. Clays

Although in recent years considerable research work was focused on the development of Nafion®-clay nanocomposite membranes mainly for DMFC applications, only few papers dealing with the Nafion® – montmorillonite (MMT) system report mechanical characterization data. Stress strain tests were carried out for recast Nafion® – organically modified MMT (Cloisite 10A) membranes, with filler loading in the range 1–15 wt%. For the membrane containing 3 wt% MMT the strength increased by more than 35% and the tensile elongation almost doubled in comparison with neat recast Nafion® [135]. Moreover, the elongation at break revealed a positive deviation for filler content up to 15 wt%, with a maximum around 3–5 wt%. This might also result from the complete dispersion or exfoliation of the clay nanolayers as shown by the X-ray pattern of the nanocomposites.

A similar behaviour was observed for Nafion® – sulfonated MMT nanocomposites produced via a film coating process using a pilot coating machine [136]. The membrane with 5 wt% filler exhibited at the same time the maximum elongation (308% versus 225% for neat Nafion®), the maximum strength and consequently the maximum thoughness (461 kJ m^{-2}versus 209 kJ m^{-2} for pristine Nafion®). Nafion–Na^+ MMT hybrid membranes with a unique microstructure [137] were synthesised using a new approach based on depletion aggregation of suspended particles – a well-known phenomenon in colloids – which occurs upon addition of a polymer to a colloidal suspension, if the polymer does not interact with the particles of the suspension. The resulting interactions can lead to particle clustering, aggregation and, in some cases, formation of a percolated network of particles, which eventually leads to gelation. Cryo-TEM images of the hybrid Nafion® – clay gels show that the clay particles in the hybrid gels form a network structure with an average cell size of 500 nm. Hybrid membranes cast from hybrid gels show significant property improvements compared to pure Nafion®, such as strongly reduced swelling in water and methanol and enhanced selectivity (ratio of conductivity over permeability) and stiffness. For example, the storage modulus of a sample containing 23 wt% clay is about 10 times that of Nafion®, while the elongation at break is by an order of magnitude lower. DMA tests, carried out from room temperature to 300 °C, show a shift of the α relaxation from ~125 °C for neat Nafion up to 230 °C. This large shift is partially attributed to an ion exchange reaction between the Nafion® and the Na^+ clay leading to the formation of the Na^+ form of Nafion, which is characterised by a similar α-relaxation temperature [138].

To further evaluate the origin of the temperature shift, a hybrid membrane was tested after acid treatment. While the relaxation shifts to lower temperature, still the transition occurs at 160 °C, which is much higher than that observed for pure Nafion®. Therefore, the large displacement of the α relaxation observed for all hybrids can be directly related to the molecular confinement in the vicinity of polymer–clay interface that drastically hinders the polymer chain motions.

Similar results were also obtained for Nafion®–MMT nanocomposite membranes that were synthesised starting from the clay in the hydrogen form [139]. Well-dispersed, mechanically robust, free-standing membranes were prepared by casting from a Nafion®-clay water suspension at 180 °C under pressure. SAXS profiles reveal a preferential orientation of Nafion aggregates parallel to the membrane surface, arising from the platelet-like shape of the clay nanoparticles, which tend to align parallel to the surface of the membrane. The nanocomposite membranes are slightly less conductive than neat Nafion®, and the difference in conductivity is more pronounced at low relative humidity and high filler loading. In terms of mechanical properties, the nanocomposite containing 20 wt% clay shows a 6-time increase in the storage modulus at 30 °C and a weak α-transition shifted around 215 °C.

5.4. Zirconium phosphate

Nafion®/zirconium phosphate ($Zr(HPO_4)_2 \cdot H_2O$, hereafter ZrP) composite membranes can be prepared by two main synthetic procedures. According to the early procedures the filler is grown within the preformed ionomer matrix by ion exchange of the ionomer protons with zirconium cationic species and subsequent membrane treatment with an aqueous solution of phosphoric acid [119,140–151]. The more recent synthetic approach is based on the coprecipitation of the filler and the ionomer from a solution containing the ionomer and a ZrP precursor [152,153]. Both procedures lead to the formation of nanometric ZrP particles with low aspect ratio and the resulting composite membranes have similar physicochemical properties: in particular, a strong decrease in the crystallinity degree of the matrix with increasing the filler concentration is observed.

The presence of ZrP results in an increase of the tensile modulus and a decrease in the peak of the tanδ vs. temperature curve with increasing ZrP loading [146,149,151,152] (Fig. 10). In the presence of water the differences in mechanical behaviour between Nafion and its composites with ZrP are progressively less evident as the water

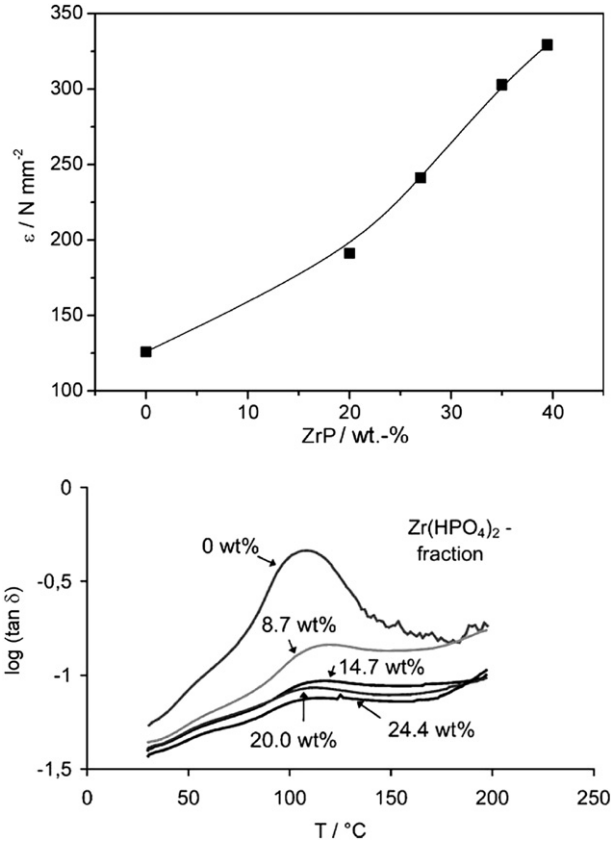

Fig. 10. Increase in elastic modulus and decrease in the peak of the tanδ vs temperature curve of Nafion with increasing ZrP content [146,151]. (Upper) Reprinted from *Fuel Cells*, Vol 8, Issues 3-4, M. Casciola, D. Capitani, A. Comite, A. Donnadio, V. Frittella, M. Pica, M. Sganappa, A. Varzi, Nafion–Zirconium Phosphate Nanocomposite Membranes with High Filler Loadings: Conductivity and Mechanical Properties, Pages 217-224, Copyright (2008), with permission from John Wiley & Sons. (Lower) Reprinted from *Journal of Membrane Science*, Vol 223, Issues 1-2, F. Bauer, M. Willert-Porada, Microstructural characterization of Zr-phosphate–Nafion® membranes for direct methanol fuel cell (DMFC) applications, Pages 141-149, Copyright (2004), with permission from Elsevier.

content increases and nearly vanish at $\lambda \approx 12$. In spite of the larger water content, the composite membranes do not show improved conductivity in comparison with Nafion® over the entire range of water activities at temperature from 80 to 140 °C [143,144,147,149,151,152] with the only exception of a composite containing 10 wt% ZrP which is slightly more conductive than Nafion for RH < 50%.

Despite this observation, the Nafion®/ZrP composites exhibit better fuel cell performance than non-modified Nafion® under high temperature and low RH conditions as reported independently by several groups [141–145]. The factors promoting improved fuel cell performance above 100 °C at RH values lower than 100% are not yet completely understood. However, it was shown that after fuel cell operation in hydrogen and oxygen at 130 °C the Nafion® 117 composite membranes underwent much less dimensional changes than pristine Nafion® 117 [148]. Treatment of Nafion/ZrP composite membranes with sulfophenylphosphonic acid leads to partial replacement of the monohydrogen phosphate group of ZrP through a topotactic anion exchange reaction. The membrane thus obtained shows improved conductivity and stiffness with respect to both Nafion® 117 and the parent composite membrane [154].The mechanical properties of Nafion/ZrP membranes are also strongly dependent on the aspect ratio of the filler particles [155]: when ZrP platelets with high aspect ratio (>20), obtained by exfoliation of microcrystalline ZrP, are used as fillers of recast Nafion®, the proportional increase of the Young's modulus is about 4 times larger than that of the composite membranes loaded with the same amount of low aspect ratio filler.

Finally, a solid state method for the preparation of Nafion®/ZrP nanocomposite membranes was recently described [156]. A nanocomposite powder from Nafion® pellets and a ZrP ceramic was formed by mechanical milling. The nanoparticles were then consolidated into membrane form by mechanical pressing. Cross-sectional analysis by scanning electron microscopy showed that the ceramic particles exist in agglomerates that are evenly dispersed across the membrane. The mechanical behaviour of the composite membranes was investigated by dynamic mechanical analysis and tensile testing. Increasing ceramic content is accompanied by an increase in the storage modulus and in the α-peak temperature. The proton conductivity of fully hydrated membranes, measured by the 4-probe method at 60 °C in water, is comparable with that of the extruded neat Nafion® membrane.

6. Summary and outlook

Many approaches have been developed for improving the mechanical properties of PFSA membranes, ranging from chemical cross-linking to physical reinforcement, each with its own advantages and disadvantages. Chemical cross-linking should in principle provide durable, chemically stable linkages, however it is often more difficult to accomplish than physical reinforcement. Most studies in this area have focused on long-side chain, Nafion® type PFSAs, with the exception of pioneering approaches at 3M [20] on the shorter side chain ionomer and recent preliminary results on chemical cross-linking of the short-side chain ionomer through perfluorobutyl functionalised precursors [36]. Much is still to be expected from a systematic investigation of the cross-linking of short-side chain PFSA such as Aquivion™, which may be a more attractive candidate for both main-chain and side-chain cross-linking due to the lower equivalent weight accessible for this ionomer and its potentially greater stability towards chemical degradation [54].

On the other hand, methods involving physical reinforcements have been much more widely investigated, probably due to their potential ease of fabrication. Thus far, the most advanced have been the use of PTFE supports such as the Gore-Select membrane, as well as various type of fabric-reinforced PFSA that have been developed for industrial electrolysis applications. The use of inert reinforcements has generally resulted in a reduction in proton conductivity, however this is compensated by greater mechanical properties which allow the use of thinner membranes and thus lower membrane area resistance. Further advancement in this area and recent results have also shown other possibilities such as the use of inorganic nanoparticles or a porous, electrospun nanofibre mat as a reinforcing matrix, allowing further functionalisation or morphological control of the reinforcing matrix to minimise the trade-off between proton conductivity and mechanical properties. Some studies have also investigated the use of materials which enhance either the proton conductivity or water retention in the membrane either as a stand-alone filler or in combination with an inert reinforcement. However, it should be pointed out that the use of inorganic fillers is generally associated with a reduction in the elongation at break which may impact the tear strength of the PFSA membrane.

Due to the complex nature of MEA degradation and the large number of variables involved, it can be difficult to produce a universal, quantifiable metric for membrane stability as both mechanical and chemical stability need to be taken into account. Current assessment of the durability of a fuel cell membrane is obtained with use of *in-situ* Accelerated Stress Testing [3] such as OCV hold test or humidity cycling, in order to obtain an estimate of the lifetime of the MEA. When it comes to individual fuel cell components such as the proton exchange membrane, however, we need to rely on *ex-situ* methods such as chemical degradation and mechanical tensile stress tests, each of which provides specific information on a particular aspect of membrane stability. Thus, it is important to have an understanding of the various parameters involved in membrane degradation and the metrics that can be used to evaluate them. Mechanical properties of a membrane such as creep resistance and storage modulus provide an indication of the puncture/tear resistance and their ability to resist morphological changes upon hydration, but such parameters also need to be evaluated in the context of polymer chemical stability in order to obtain a true indication of membrane durability in an operating fuel cell.

In light of this, both chemical and mechanical stabilisation methods are required to obtain a synergistic effect, with the specific methods carefully adapted towards addressing particular challenges (e.g. high temperature operation, use of liquid fuels) in order to obtain the best-performing material as the requirements differ amongst the various applications. As many factors related to both the material (mechanical strength, durability, stability) and fabrication method (morphology, pore-filling) are important to the final product, new or improved support materials and novel fabrication techniques are essential to achieving a membrane with high strength and durability without compromising fuel cell performance.

Acknowledgment

This work was partially supported by funding under the FCH-JU MAESTRO project, contract number 256647.

References

[1] R. Devanathan, Energy Environ. Sci. 1 (2008) 101–119.
[2] K.A. Mauritz, R.B. Moore, Chem. Rev. 104 (2004) 4535–4585.
[3] R. Borup, J. Meyers, B. Pivovar, Y.S. Kim, R. Mukundan, N. Garland, D. Myers, M. Wilson, F. Garzon, D. Wood, P. Zelenay, K. More, K. Stroh, T. Zawodzinski, J. Boncella, J.E. McGrath, M. Inaba, K. Miyatake, M. Hori, K. Ota, Z. Ogumi, S. Miyata, A. Nishikata, Z. Siroma, Y. Uchimoto, K. Yasuda, K.-i. Kimijima, N. Iwashita, Chem. Rev. 107 (2007) 3904–3951.
[4] X. Huang, R. Solasi, Y. Zou, M. Feshler, K. Reifsnider, D. Condit, S. Burlatsky, T. Madden, J. Polym. Sci. Part B Polym. Phys. 44 (2006) 2346–2357.

[5] S.C. Yeo, A. Eisenberg, J. Appl. Polym. Sci. 21 (1977) 875.
[6] K.A. Page, K.M. Cable, R.B. Moore, Macromolecules 38 (2005) 6472.
[7] S.J. Osborn, M.K. Hassan, D.W. Rhodes, K.A. Mauritz, R.B. Moore, Macromolecules 40 (2007) 3886–3890.
[8] S. Kundu, L.C. Simon, M. Fowler, S. Grot, Polymer 46 (2005) 11707–11715.
[9] K. Patankar, D. David, M. Ellis, C. Scott, Y.-H. Lai, C.S. Gittleman, Fuel Cells 12 (2012) 787–799.
[10] Y. Li, D.A. Dillard, Y.-H. Lai, S.W. Case, M.W. Ellis, M.K. Budinski, C.S. Gittleman, J. Electrochem. Soc. 159 (2012) B173–B184.
[11] J. Wu, X.Z. Yuan, J.J. Martin, H. Wang, J. Zhang, J. Shen, S. Wu, W. Merida, J. Power Sources 184 (2008) 104–119.
[12] A. Collier, H. Wang, X.Z. Yuan, J. Zhang, D.P. Wilkinson, Int. J. Hydrogen Energy 31 (2006) 1838–1854.
[13] A. Kusoglu, M.H. Santare, A.M. Karlsson, J. Polym. Sci. Part B Polym. Phys. 49 (2011) 1506–1517.
[14] Y. Li, D.A. Dillard, S.W. Case, M.W. Ellis, Y.-H. Lai, C.S. Gittleman, D.P. Miller, J. Power Sources 194 (2009) 873–879.
[15] R.C. McDonald, C.K. Mittlesteadt, E.L. Thompson, Fuel Cells 4 (2004) 208–213.
[16] D. Wu, S.J. Paddison, J.A. Elliott, Energy Environ. Sci. 1 (2008) 284–293.
[17] A. Kusoglu, A.M. Karlsson, M.H. Santare, S. Cleghorn, W.B. Johnson, J. Power Sources 170 (2007) 345–358.
[18] A. Kusoglu, M.H. Santare, A.M. Karlsson, S. Cleghorn, W.B. Johnson, J. Electrochem. Soc. 157 (2010) B705–B713.
[19] D. Schiraldi, J. Macromol. Sci. Part C Polym. Rev. 46 (2006) 315–327.
[20] S. Hamrock, M.A. Yandrasits, J. Macromol. Sci. Part C Polym. Rev. 46 (2006) 219–244.
[21] W. Ma, C. Zhao, J. Yang, J. Ni, S. Wang, N. Zhang, H. Lin, J. Wang, G. Zhang, Q. Li, H. Na, Energy Environ. Sci. 5 (2012) 7617–7625.
[22] M.J. Covitch, S.R. Lowry, C.L. Gray, B. Blackford, Polym. Sci. Technol. (Polym. Sep. Media) 16 (1982) 257–267.
[23] C.J. Hora, D.E. Maloney, Electrochem. Soc. Ext. Abstr. 77 (1977) 1145.
[24] D.D. DesMarteau, J. Fluor. Chem. 72 (1995) 203–208.
[25] L.A. Ford, D.D. DesMarteau, D.W. S Jr., J. Fluor. Chem. 126 (2005) 653–660.
[26] S.C. Savett, J.R. Atkins, C.R. Sides, J.L. Harris, B.H. Thomas, S.E. Creager, W.T. Pennington, D.D. DesMarteau, J. Electrochem. Soc. 149 (2002) A1527.
[27] N. Uematsu, N. Hoshi, T. Koga, M. Ikeda, J. Fluor. Chem. 127 (2006) 1087–1095.
[28] Y.M. Zhang, L. Li, J.K. Tang, B. Bauer, W. Zhang, H.R. Gao, M. Taillades-Jacquin, D.J. Jones, J. Rozière, N. Lebedeva, R.K.A.M. Mallant, ECS Trans. 25 (2009) 1469–1472.
[29] K. Xu, C.S. Ewing, M.A. Hickner, Q. Wang, Macromolecules 43 (2010) 1692–1694.
[30] A.J. Greso, R.B. Moore, K.M. Cable, W.L. Jarrett, K.A. Mauritz, Polymer 38 (1997) 1345–1356.
[31] L. Sauguet, B. Ameduri, B. Boutevin, J. Polym. Sci. Part A Polym. Chem. 44 (2006) 4566–4578.
[32] S. Hamrock (2008) http://www.hydrogen.energy.gov/pdfs/review08/fc_13_hamrock.pdf, Last accessed 20/01 2012.
[33] S. Hamrock (2010) http://www.hydrogen.energy.gov/pdfs/review10/fc034_hamrock_2010_o_web.pdf, Last accessed 20/01 2012.
[34] M.A. Yandrasits, S.J. Hamrock, K. Hintzer, U.S. Patent, 20,050,107,490 A1, 3M Innovative Properties Company (2005).
[35] M.A. Yandrasits, S.J. Hamrock, S.J. Grootaert, U.S. Patent, 20,050,107,489 A1, 3M Innovative Properties Company (2005).
[36] H. Gao, PhD Thesis, Université Montpellier 2, (2010) Available on http://www.biu-montpellier.fr/florabium/jsp/nnt.jsp?nnt=2010MON20236, Last accessed 21/01/2013.
[37] B. Bae, H.Y. Ha, D. Kim, J. Membr. Sci. 276 (2006) 51–58.
[38] D.E. Curtin, R.E. Lousenberg, T.J. Henry, P. Tangeman, M.E. Tisack, J. Power Sources 131 (2004) 41–48.
[39] K.E. Schwiebert, K.G. Raiford, G. Escobedo, G. Nagarajan, ECS Trans. 1 (2006) 303–311.
[40] F.D. Coms, ECS Trans. 16 (2008) 235–255.
[41] V. Ramani, H.R. Kunz, J.M. Fenton, J. Power Sources 152 (2005) 182–188.
[42] P. Trogadas, J. Parrondo, F. Mijangos, V. Ramani, J. Mater. Chem. 21 (2011) 19381–19388.
[43] P. Trogadas, J. Parrondo, V. Ramani, ACS Symposium Series, 1034 (2010) 187–207.
[44] M.H. Frey, D.M. Pierpont, S.J. Hamrock, WO Patent, WO2007120189, 3M Innovative Properties Company (2007).
[45] E. Endoh, WO Patent, WO2006006357, Asahi Glass Company Ltd. (2006).
[46] N.R. Andrews, S.D. Knights, K.A. Murray, S.J. McDermid, S.M. MacKinnon, S. Ye, US Patent, 7,537,857, BDF IP Holdings Ltd. (2009).
[47] F.D. Coms, J.E. O'Hara, US Patent, 2008/0107,945, GM Global Technology Operations LLC (2006).
[48] E. Endoh, ECS Trans. 25 (2010) 293–307.
[49] E. Endoh, ECS Trans. 16 (2008) 1229–1240.
[50] J. Zhang, B. Litteer, F.D. Coms, R. Makharia, ECS Trans. 41 (2011) 1471–1485.
[51] F.D. Coms, H. Liu, J.E. Owejan, ECS Trans. 16 (2008) 1735–1747.
[52] G.M. Haugen, F. Meng, N. Aieta, J.L. Horan, M.-C. Kuo, M.H. Frey, S.J. Hamrock, A.M. Herring, Electrochem. Solid State Lett. 10 (2007) B51–B55.
[53] S. Xiao, H. Zhang, C. Bi, Y. Zhang, Y. Ma, X. Li, H. Zhong, Y. Zhang, J. Power Sources 195 (2010) 8000–8005.
[54] M. Danilczuk, A.J. Perkowski, S. Schlick, Macromolecules 43 (2010) 3352–3358.
[55] R.B. Moore, C.R. Martin, Anal. Chem. 58 (1986) 2569–2570.
[56] G. Gebel, P. Aldebert, M. Pineri, Macromolecules 20 (1987) 1425–1428.
[57] A.E. Steck, C. Stone, U.S. Patent, 5,834,523, Ballard Power Systems, Inc (1998).
[58] J.E. Spethmann, J.T. Keating, W.O. Patent, 9850457A1, E.I. du Pont de Nemours and Company (1998).
[59] B. Bahar, A.R. Hobson, J. Kolde, U.S. Patent, 5,547,551, Gore Enterprise Holdings, Inc (1996).
[60] S. Banerjee, J.D. Summers, W.O. Patent, 9851733A1, E.I. du Pont de Nemours and Company (1998).
[61] R.M. Penner, C.R. Martin, J. Electrochem. Soc. 132 (1985) 514.
[62] C. Liu, C.R. Martin, J. Electrochem. Soc. 137 (1990) 510.
[63] C. Liu, C.R. Martin, J. Electrochem. Soc. 137 (1990) 3114.
[64] K.M. Nouel, P.S. Fedkiw, Electrochim. Acta 43 (1998) 2381–2387.
[65] M.W. Verbrugge, R.F. Hill, E.W. Schneider, AIChE J. 38 (1992) 93–100.
[66] H. Dhar, U.S. Patent, 5,242,764, BCS Technology, Inc. (1993).
[67] B. Bahar, A.R. Hobson, J.A. Kolde, D. Zuckerbrod, U.S. Patent, 5,547,551, Gore Enterprise Holdings, Inc. (1996).
[68] T.R. Ralph, D.E. Barnwell, P.J. Bouwman, A.J. Hodgkinson, M.I. Petch, M. Pollington, J. Electrochem. Soc. 155 (2008) B411–B422.
[69] J. Shim, H.Y. Ha, S. Hong, I. Oh, J. Power Sources 109 (2002) 412.
[70] H. Tang, X. Wang, M. Pan, F. Wang, J. Membr. Sci. 306 (2007) 298–306.
[71] Y. Higuchi, N. Terada, H. Shimoda, S. Hommura, U.S. Patent Application, 0026883A1, Asahi Glass Company, Ltd. (2001).
[72] C.A. Koval, T. Spontarelli, P. Thoen, R.D. Noble, Ind. Eng. Chem. Res. 31 (1992) 1116.
[73] G.G. Kumar, D.N. Lee, P. Kim, K.S. Nahma, R.N. Elizabeth, Eur. Polym. J. 44 (2008) 2225.
[74] S. Haufe, U. Stimming, J. Membr. Sci. 185 (2001) 95–103.
[75] J. Shin, B. Chang, J. Kim, S. Lee, D.H. Suh, J. Membr. Sci. 251 (2005) 247–254.
[76] D.M. Xing, B.L. Yi, F.Q. Liu, Y.Z. Fu, H.M. Zhang, Fuel Cells 5 (2005) 406–411.
[77] J.A. Kolde, B. Bahar, M.S. Wilson, T.A. Zawodzinski, S. Gottesfeld, in: S. Gottesfeld, G. Halpert, A. Landgrebe (Eds.), Proceedings of the 1st International Symposium on Proton Conducting Membrane Fuel Cells, Electrochemical Society, Inc, Pennington, NJ, 1995, pp. 193–201.
[78] W. Liu, K. Ruth, G.J. Rusch, New Mater. Electrochem. Syst. 4 (2001) 227.
[79] W. Grot, Fluorinated Ionomers, second ed., Elsevier, Oxford, 2011.
[80] S. Banerjee, D. Prugh, S. Frisk, ECS Trans. 50 (2012) 887–895.
[81] Y. Tang, A. Kusoglu, A.M. Karlsson, M.H. Santare, S. Cleghorn, W.B. Johnson, J. Power Sources 175 (2008) 817–825.
[82] W. Liu, T. Suzuki, H. Mao, T. Schmiedel, ECS Trans. 50 (2012) 51.
[83] H. Tang, M. Pan, F. Wang, P.K. Shen, S.P. Jiang, J. Phys. Chem. B 111 (2007) 8684–8690.
[84] F. Liu, B. Yi, D. Xing, J. Yu, H. Zhang, J. Membr. Sci. 212 (2003) 213–223.
[85] H. Tang, M. Pan, S.P. Jiang, X. Wang, Y. Ruan, Electrochim. Acta 52 (2007) 5304–5311.
[86] O. Savadogo, J. New Mater. Electrochem. 1 (1998) 47.
[87] M.P. Rodgers, J. Berring, S. Holdcroft, Z. Shi, J. Membr. Sci. 321 (2008) 100–113.
[88] S.-Y. Ahn, Y.-C. Lee, H.Y. Ha, S.-A. Hong, I.-H. Oh, Electrochim. Acta 50 (2004) 571–575.
[89] H. Suzuki, European Patent, 2037521A1, Toyota (2007).
[90] S. Hommura, Y. Kunisa, I. Terada, M. Yoshitake, J. Fluor. Chem. 120 (2003) 151–155.
[91] M. Yoshitake, E. Yanagisawa, T. Naganuma, Y. Kunisa, Mat. Res. Soc. Symp. Proc. 575 (2000) 213–227.
[92] H.-L. Lin, T.-J. Chang, J. Membr. Sci. 325 (2008) 880–886.
[93] Y. Liu, T. Nguyen, N. Kristian, Y. Yu, X. Wang, J. Membr. Sci. 330 (2009) 357–362.
[94] L. Tchicaya-Bouckary, D.J. Jones, J. Roziere, Fuel Cells 2 (2002) 240–245.
[95] J. Rozière, D.J. Jones, in: W. Vielstich, A. Lamm, H. Gasteiger (Eds.), Handbook of Fuel Cells, John Wiley and Sons, 2003, pp. 447–455.
[96] Z.Q. Tian, S.P. Jiang, Z. Liu, L. Li, Electrochem. Commun. 9 (2007) 1613–1618.
[97] T. Nguyen, X. Wang, J. Power Sources 195 (2010) 1024–1030.
[98] M.H. Yildirim, D. Stamatialis, M. Wessling, J. Membr. Sci. 321 (2008) 364–372.
[99] J.H. Shim, I.G. Koo, W.M. Lee, Electrochim. Acta 50 (2005) 2385–2391.
[100] H. Pan, H. Pu, D. Wan, M. Jin, Z. Chang, J. Power Sources 195 (2010) 3077–3083.
[101] B. Zhou, H. Pu, H. Pan, D. Wan, Int. J. Hydrogen Energy 36 (2011) 6809–6816.
[102] H. Pan, H. Pu, M. Jin, D. Wan, Z. Chang, Polymer 51 (2010) 2305–2312.
[103] V. Thavasi, G. Singh, S. Ramakrishna, Energy Environ. Sci. 1 (2008) 205.
[104] S. Cavaliere, S. Subianto, I. Savych, D.J. Jones, J. Roziere, Energy Environ. Sci. 4 (2011) 4761–4785.
[105] S.W. Choi, Y.Z. Fu, Y.R. Ahn, S.M. Jo, A. Manthiram, J. Power Sources 180 (2008) 167–171.
[106] S. Molla, V. Compan, J. Membr. Sci. 372 (2011) 191–200.
[107] S. Molla, V. Compan, J. Power Sources 196 (2011) 2699–2708.
[108] H.L. Lin, S.H. Wang, C.K. Chiu, T.L. Yu, L.C. Chen, C.C. Huang, T.H. Cheng, J.M. Lin, J. Membr. Sci. 365 (2010) 114–122.
[109] N.W. DeLuca, Y.A. Elabd, J. Power Sources 163 (2006) 386–391.
[110] I. Shabani, M.M. Hasani-Sadrabadi, V. Haddadi-Asl, M. Soleimani, J. Membr. Sci. 368 (2011) 233–240.
[111] M.M. Hasani-Sadrabadi, I. Shabani, M. Soleimani, H. Moaddel, J. Power Sources 196 (2011) 4599–4603.
[112] H. Hwang, H.Y. Lee, S. Park, S. Choi, Y.-g. Shul, in: 217th ECS Meeting, Vancouver, 2010.

[113] J.-R. Lee, N.-Y. Kim, M.-S. Lee, S.-Y. Lee, J. Membr. Sci. 367 (2011) 265–272.
[114] H. Chen, J.D. Snyder, Y.A. Elabd, Macromolecules 41 (2008) 128–135.
[115] A. Laforgue, L. Robitaille, A. Mokrini, A. Ajji, Macromol. Mater. Eng. 292 (2007) 1229–1236.
[116] J. Choi, K.M. Lee, R. Wycisk, P.N. Pintauro, P.T. Mather, J. Mater. Chem. 20 (2010) 6282–6290.
[117] S. Subianto, S. Cavaliere, D.J. Jones, J. Rozière, J. Polym. Sci. Part A Polym. Chem. 51 (2013) 118–128.
[118] J. Choi, K.M. Lee, R. Wycisk, P.N. Pintauro, P.T. Mather, ECS Trans. 16 (2008) 1433–1442.
[119] D.J. Jones, J. Rozière, Adv. Polym. Sci. 215 (2008) 219–264.
[120] Y.H. Liu, B.L. Yi, Z.G. Shao, D.M. Xing, H.M. Zhang, Electrochem. Solid State Lett. 9 (2006) A356–A359.
[121] L. Wang, D.M. Xing, H.M. Zhang, H.M. Yu, Y.H. Liu, B.L. Yi, J. Power Sources 176 (2008) 270–275.
[122] J.M. Thomassin, J. Kollar, G. Caldarella, A. Germain, R. Jerome, C. Detrembleur, J. Membr. Sci. 303 (2007) 252–257.
[123] N.P. Cele, S.S. Ray, S.K. Pillai, M. Ndwandwe, S. Nonjola, L. Sikhwivhilu, M.K. Mathe, Fuel Cells 10 (2010) 64–71.
[124] S.K. Young, K.A. Mauritz, J.Polym. Sci. Part B Polym. Phys. 39 (2001) 1282–1295.
[125] Q. Deng, R.B. Moore, K.A. Mauritz, J. Appl. Polym. Sci. 68 (1998) 747–763.
[126] Y. Patil, K.A. Mauritz, J. Appl. Polym. Sci. 113 (2009) 3269–3278.
[127] V.Di Noto, R. Gliubizzi, E. Negro, G. Pace, J. Phys. Chem. B. 110 (2006) 24972–24986.
[128] S. Thayumanasundaram, M. Piga, S. Lavina, E. Negro, M. Jeyapandian, L. Ghassemzadeh, K.J. Müller, V.Di Noto, Electrochim. Acta 55 (2010) 1355–1365.
[129] S. Mulmi, C.H. Park, H.K. Kim, C.H. Lee, H.B. Park, Y.M. Lee, J. Membr. Sci. 344 (2009) 288–296.
[130] J. Yuan, H. Pu, Z. Yang, J. Polym. Sci. Part A Polym. Chem. 47 (2009) 2647–2655.
[131] M.B. Satterfield, P.W. Majsztrik, H. Ota, J.B. Benziger, A.B. Bocarsly, J. Polym. Sci. Part B Polym. Phys. 44 (2006) 2327–2345.
[132] V.Di Noto, S. Lavina, E. Negro, M. Vittadello, F. Conti, M. Piga, G. Pace, J. Power Sources 187 (2009) 57–66.
[133] V.Di Noto, N. Boaretto, E. Negro, G. Pace, J. Power Sources 195 (2010) 7734–7742.
[134] X. Zhang, S.W. Tay, L. Hong, Z. Liu, J. Membr. Sci. 320 (2008) 310–318.
[135] M.K. Song, S.B. Park, Y.T. Kim, K.H. Kim, S.K. Min, H.W. Rhee, Electrochim. Acta 50 (2004) 639–643.
[136] T.K. Kim, M. Kang, Y.S. Choi, H.K. Kim, W. Lee, H. Chang, D. Seung, J. Power Sources 165 (2007) 1–8.
[137] E. Burgaz, H. Lian, R. Alonso, L. Estevez, A. Kelarakis, E.P. Giannelis, Polymer 50 (2009) 2384–2392.
[138] K.M. Cable, in: The University of Southern Mississippi, Hattiesburg, 1996.
[139] R.H. Alonso, L. Estevez, H. Lian, A. Kelarakis, E.P. Giannelis, Polymer 50 (2009) 2402–2410.
[140] W. Grot, G. Rajendran, WO Patent, WO9629752 (1996).
[141] C. Yang, S. Srinivasan, A.S. Aricò, P. Creti, V. Baglio, V. Antonucci, Electrochem. Solid State Lett. 4 (2001) A31–A34.
[142] C. Yang, P. Costamagna, S. Srinivasan, J. Benziger, A.B. Bocarsly, J. Power Sources 103 (2001) 1–9.
[143] P. Costamagna, C. Yang, A.B. Bocarsly, S. Srinivasan, Electrochim. Acta 47 (2002) 1023–1033.
[144] C. Yang, S. Srinivasan, A.B. Bocarsly, S. Tulyani, J.B. Benziger, J. Membr. Sci. 237 (2004) 145–161.
[145] H.-K. Lee, J.-I. Kim, J.-H. Park, T.-H. Lee, Electrochim. Acta 50 (2004) 761–768.
[146] F. Bauer, M. Willert-Porada, J. Membr. Sci. 233 (2004) 141–149.
[147] F. Bauer, M. Willert-Porada, J. Power Sources 145 (2005) 101–107.
[148] F. Bauer, M. Willert-Porada, Fuel Cells 6 (2006) 261–269.
[149] F. Bauer, M. Willert-Porada, Solid State Ionics 177 (2006) 2391–2396.
[150] F. Bauer, A. Müller, A. Wojtkowiak, M. Willert-Porada, Adv. Sci. Technol. 45 (2006) 787–792.
[151] M. Casciola, D. Capitani, A. Comite, A. Donnadio, V. Frittella, M. Pica, M. Sganappa, A. Varzi, Fuel Cells 8 (2008) 217–224.
[152] G. Alberti, M. Casciola, D. Capitani, A. Donnadio, R. Narducci, M. Pica, M. Sganappa, Electrochim. Acta 52 (2007) 8125–8132.
[153] G. Alberti, M. Casciola, A. Donnadio, R. Narducci, M. Pica, M. Sganappa, Desalination 199 (2006) 280–282.
[154] M. Casciola, D. Capitani, A. Donnadio, V. Frittella, M. Pica, M. Sganappa, Fuel Cells 9 (2009) 381–386.
[155] M. Casciola, G. Bagnasco, A. Donnadio, L. Micoli, M. Pica, M. Sganappa, M. Turco, Fuel Cells 9 (2009) 394–400.
[156] A.L. Moster, B.S. Mitchell, J. Appl. Polym. Sci. 111 (2009) 1144–1150.
[157] DuPont (2009) http://www2.dupont.com/FuelCells/en_US/assets/downloads/dfc101.pdf, Last accessed 05/03 2012.
[158] C.S. Gittleman, Y.-H. Lai, D.P. Miller, in: AIChE Annual Meeting, Cincinnati, OH, 2005.
[159] SolvaySolexis (2012) http://www.solvayplastics.com/sites/solvayplastics/EN/specialty_polymers/Pages/DataSheets.aspx, Last accessed 06/03 2012.